



39 Abstract

40 The Land Surface, Snow and Soil Moisture Model Intercomparison Project (LS3MIP) is
41 designed to provide a comprehensive assessment of land surface, snow, and soil moisture
42 feedbacks on climate variability and climate change, and to diagnose systematic biases in
43 the land modules of current Earth System Models (ESMs). The solid and liquid water stored
44 at the land surface has a large influence on the regional climate, its variability and
45 predictability, including effects on the energy, water and carbon cycles. Notably, snow and
46 soil moisture affect surface radiation and flux partitioning properties, moisture storage and
47 land surface memory. They both strongly affect atmospheric conditions, in particular
48 surface air temperature and precipitation, but also large-scale circulation patterns.
49 However, models show divergent responses and representations of these feedbacks as well
50 as systematic biases in the underlying processes. LS3MIP will provide the means to quantify
51 the associated uncertainties and better constrain climate change projections, which is of
52 particular interest for highly vulnerable regions (densely populated areas, agricultural
53 regions, the Arctic, semi-arid and other sensitive terrestrial ecosystems).

54 The experiments are subdivided in two components, the first addressing systematic land
55 biases in offline mode ("LMIP", building upon the 3rd phase of Global Soil Wetness Project;
56 GSWP3) and the second addressing land feedbacks attributed to soil moisture and snow in
57 an integrated framework ("LFMIP", building upon the GLACE-CMIP blueprint).

58

59 Introduction

60 Land surface processes, including heat fluxes, snow, soil moisture, vegetation, turbulent
61 transfer and runoff, continue to be ranked highly on the list of the most relevant yet
62 complex and poorly represented features in state-of-the-art climate models. People live on
63 land, exploit its water and natural resources, and experience day-to-day weather that is
64 strongly affected by feedbacks with the land surface. The six Grand Challenges of the World
65 Climate Research Program (WCRP)¹ include topics governed primarily (Water Availability,
66 Cryosphere) or largely (Climate Extremes) by land surface characteristics.

67 Despite the importance of a credible representation of land surface processes in Earth
68 System Models (ESMs), a number of systematic biases and uncertainties persist. Biases in
69 hydrological characteristics (e.g. moisture storage in soil and snow, runoff, vegetation and
70 surface water bodies), partitioning of energy and water fluxes (Seneviratne et al. 2010),
71 definition of initial and boundary conditions at the appropriate spatial scale, feedback
72 strengths (Koster et al. 2004; Qu and Hall 2014) and inherent land surface related
73 predictability (Douville et al. 2007; Dirmeyer et al. 2013) are still subjects of considerable
74 research effort.

75 These biases and uncertainties are problematic, because they affect, among others, forecast
76 skill (Koster et al. 2010a), regional climate change patterns (Campoy et al. 2013; Seneviratne

¹ <http://www.wcrp-climate.org/grand-challenges>



77 et al. 2013; Koven et al. 2012), and explicable trends in water resources (Lehning 2013). In
78 addition, there is evidence of the presence of large-scale systematic biases in some aspects
79 of land hydrology in current climate models (Mueller and Seneviratne 2014) and the
80 terrestrial component of the carbon cycle (Anav et al. 2013; Mystakidis et al. 2016). Notably,
81 land surface processes can be an important reason for a direct link between the climate
82 models' temperature biases in the present period and in the future projections with
83 increased radiative forcings at the regional scale (Cattiaux et al. 2013).

84 For snow cover, a better understanding of the links with climate is critical for interpretation
85 of the observed dramatic reduction in springtime snow cover over recent decades (e.g.
86 (Derksen and Brown 2012; Brutel-Vuilmet et al. 2013), to improve the seasonal to
87 interannual forecast skill of temperature, runoff and soil moisture (e.g. Thomas et al. 2015;
88 Peings et al. 2011), and to adequately represent polar warming amplification in the Arctic
89 (e.g. Holland and Bitz, 2003). Snow-related biases in climate models may arise from the
90 snow-albedo feedback (Qu and Hall 2014; Thackeray et al. 2015a), but also from the energy
91 sink induced by snow melting in spring and the thermal insulation effect of snow on the
92 underlying soil (Koven et al. 2012; Gouttevin et al. 2012). Phase 1 and 2 of the Snow Model
93 Intercomparison Project (SnowMIP) (Etchevers et al. 2004; Essery et al. 2009) provided
94 useful insights in the capacity of snow models of different complexity to simulate the
95 snowpack evolution from local meteorological forcing but did not explore snow-climate
96 interactions. Because of strong snow/atmosphere interactions, it remains difficult to
97 distinguish and quantify the various potential causes for disagreement between observed
98 and modeled snow trends and the related climate feedbacks.

99 Soil moisture plays a central role in the coupled land – vegetation – snow – water –
100 atmosphere system (Seneviratne et al., 2010; van den Hurk et al., 2011), where interactions
101 are evident at many relevant time scales: diurnal cycles of land surface fluxes, (sub-
102)seasonal predictability of droughts, floods, and hot extremes, annual cycles governing the
103 water buffer in dry seasons, and shifts in the climatology in response to changing patterns of
104 precipitation and evaporation. The representation of historical variations in land water
105 availability and droughts still suffer from large uncertainties, due to model
106 parameterizations, unrepresented hydrologic processes such as lateral groundwater flow,
107 lateral flows connected to reinfiltration of river water or irrigation with river water, and/or
108 atmospheric forcings (Sheffield et al. 2012; Zampieri et al. 2012); Trenberth et al. 2014;
109 Greve et al. 2014; Clark et al. 2015). This also applies to the energy and carbon exchanges
110 between the land and the atmosphere (e.g. Mueller and Seneviratne 2014; Friedlingstein et
111 al. 2013).

112 It is difficult to generate reliable observations of soil moisture and land surface fluxes that
113 can be used as boundary conditions for modelling and predictability studies. Satellite
114 retrievals, in situ observations, offline model experiments (Second Global Soil Wetness
115 Project, GSWP2; Dirmeyer et al. 2006) and indirect estimates all have a potential to
116 generate relevant information but are largely inconsistent, covering different model
117 components, and suffer from methodological flaws (Mueller et al. 2013; Jiafu Mao et al.
118 2015). As a consequence, the pioneering work on deriving soil moisture related land-



119 atmosphere coupling strength (Koster et al. 2004) and regional/global climate responses in
120 both present and future climate (Seneviratne et al. 2006, 2013) has been carried out using
121 (ensembles of) modelling experiments. The second Global Land Atmosphere Coupling
122 Experiment (GLACE2; Koster et al., 2010a) measured the actual temperature and
123 precipitation skill improvement of using GSWP2 soil moisture initializations, which is much
124 lower than suggested by the coupling strength diagnostics. Limited quality of the initial
125 states, limited predictability and poor representation of essential processes determining the
126 propagation of information through the hydrological cycle in the models all play a role.

127 Altogether, there are substantial challenges concerning both the representation of land-
128 surface processes in current-generation ESMs and the understanding of related climate
129 feedbacks. The Land Surface, Snow and Soil moisture Model Intercomparison Project
130 (LS3MIP) is designed to allow the climate modelling community to make substantial
131 progress in addressing these challenges. It is part of the sixth phase of the Coupled Model
132 Intercomparison Project (CMIP6; Eyring et al. 2015). The following section further develops
133 the objectives and rationale of LS3MIP. The experimental design and analysis plan is
134 presented thereafter. The final discussion section describes the expected outcome and
135 impact of LS3MIP.

136

137 **Objectives and rationale**

138 The goal of the collection of LS3MIP experiments is to provide a comprehensive assessment
139 of land surface, snow, and soil moisture-climate feedbacks, and to diagnose systematic
140 biases and process-level deficiencies in the land modules of current ESMs. It will provide the
141 means to quantify the associated uncertainties and better constrain climate change
142 projections, of particular interest for highly vulnerable regions (including densely populated
143 regions, the Arctic, agricultural areas, and some terrestrial ecosystems).

144 The LS3MIP experiments collectively address the following objectives:

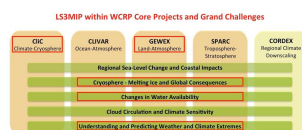
- 145 • evaluate the current state of land processes including surface fluxes, snow cover and
146 soil moisture representation in CMIP DECK (Diagnostic, Evaluation and Characterization of
147 Klima) experiments and CMIP6 historical simulations (Eyring et al. 2015), to identify the
148 main systematic biases and their dependencies;
- 149 • estimate multi-model long-term terrestrial energy/water/carbon cycles, using the
150 land modules of CMIP6 models under observation-constrained historical (land reanalysis)
151 and projected future (impact assessment) climatic conditions considering land use/land
152 cover changes;
- 153 • assess the role of snow and soil moisture feedbacks in the regional response to
154 altered climate forcings, focusing on controls of climate extremes, water availability and
155 high-latitude climate in historical and future scenario runs;
- 156 • assess the contribution of land surface processes to systematic Earth System model
157 biases and the current and future predictability of regional temperature/precipitation
158 patterns.



159 These objectives address each of the three CMIP6 overarching questions: 1) What are
160 regional feedbacks and responses to climate change?; 2) What are the systematic biases in
161 the current climate models?; and 3) What are the perspectives concerning the generation of
162 predictions and scenarios?

163 LS3MIP encompasses a family of model experiments building on earlier multi-model
164 experiments, particularly a) offline land surface experiments (GSWP2 and its successor
165 GSWP3), b) the coordinated snow model intercomparisons SnowMIP phase 1 and 2
166 (Etchevers et al., 2002; Essery et al., 2009), and c) the coupled climate time-scale GLACE-
167 type configuration (GLACE-CMIP, Seneviratne et al. 2013). Within LS3MIP the Land-only
168 experimental suite is referred to as **LMIP (Land Model Intercomparison Project)** with the
169 experiment ID **Land**, while the coupled suite is labelled as **LFMIP (Land Feedback MIP)**. A
170 detailed description of the model design is given below, and a graphical display of the
171 various components within LS3MIP is shown in Figure 3.

172



173

174 *Figure 1: Relevance of LS3MIP for WCRP Core Projects and Grand Challenges²*

175

176 As illustrated in Figure 1, LS3MIP is addressing multiple WCRP Grand Challenges and core
177 projects and is therefore relevant for a large fraction of the WCRP activities. It is initiated by
178 two out of four WCRP core projects (CLIC and GEWEX) and directly related to three WCRP
179 Grand Challenges (Cryosphere in a Changing Climate, Changes in Water Availability, and
180 Climate Extremes). The LMIP experiment will provide better estimates of historical changes
181 in snow and soil moisture at global scale, thus allowing the evaluation of changes in
182 freshwater, agricultural drought, and streamflow extremes over continents, and a better
183 understanding of the main drivers of these changes. The LFMIP experiments are of high
184 relevance for the assessment of key feedbacks and systematic biases of land surfaces
185 processes in coupled mode, and are particularly focusing on two of the main feedback loops
186 over land: the snow-albedo-temperature feedback involved in Arctic Amplification, and the
187 soil moisture-temperature feedback leading to major changes in temperature extremes
188 (Douville et al. 2016). In addition, LS3MIP will allow the exchange of data and knowledge
189 across the snow and soil moisture research communities that address a common physical
190 topic: terrestrial water in liquid and solid form. Snow and soil moisture dynamics are often
191 interrelated (e.g. Hall et al. 2008) and jointly contribute to hydrological variability (e.g.
192 Koster et al. 2010b).

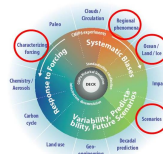
193 LS3MIP will also provide relevant insights for other research communities within WCRP,
194 such as global reconstructions of land variables that are not directly observed for detection

² <http://wcrp-climate.org/index.php/grand-challenges>; status Dec 2015



195 and attribution studies (Douville et al. 2013), estimates of freshwater inputs to the oceans
 196 (which are relevant for sea-level changes and regional impacts; Carmack et al. 2015), the
 197 assessment of feedbacks shown to strongly modulate regional climate variability relevant
 198 for regional climate information, as well as the investigation of land climate feedbacks on
 199 large-scale circulation patterns and cloud occurrence (Zampieri and Lionello 2011). This will
 200 thus also imply potential contributions to the other WCRP Grand Challenges and core
 201 projects and to programmes like the Inter-Sectoral Impact Model Intercomparison Project
 202 (ISIMIP; Warszawski et al. 2014) and the International Detection and Attribution Group
 203 IDAG.

204

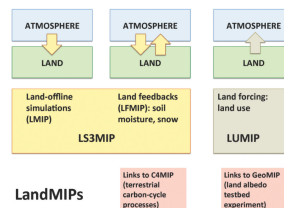


205

206 *Figure 2: Embedding of LS3MIP within CMIP6. Adapted from Eyring et al. (2015)*

207

208 Figure 2 illustrates the embedding of LS3MIP within CMIP6. LS3MIP fills a major gap by
 209 considering systematic land biases and land feedbacks. In this context, LS3MIP is part of a
 210 larger “LandMIP” series of CMIP6 experiments fully addressing biases, uncertainties,
 211 feedbacks and forcings from the land surface (Figure 3), which are complementary to similar
 212 experiments for ocean or atmospheric processes (Seneviratne et al. 2014). In particular, we
 213 note that while LS3MIP focuses on systematic biases in land surface processes (Land) and on
 214 feedbacks from the land surface processes on the climate system (LFMIP), the
 215 complementary Land Use MIP (LUMIP) experiment addresses the role of land use forcing on
 216 the climate system. The role of vegetation and carbon stores in the climate system is a point
 217 of convergence between LUMIP and LS3MIP, and the offline LMIP experiment will serve as
 218 land-only reference experiments for both the LS3MIP and LUMIP experiments. In addition,
 219 there will also be links to the C4MIP experiment with respect to impacts of snow and soil
 220 moisture processes (in particular droughts and floods) on terrestrial carbon exchanges and
 221 resulting feedbacks to the climate system.



222

223 *Figure 3: Structure of the “LandMIPs”. LS3MIP includes (1) the offline representation of land*
 224 *processes (LMIP) and (2) the representation of land-atmosphere feedbacks related to snow*
 225 *and soil moisture (LFMIP). Forcing associated with land use is assessed in LUMIP. Substantial*

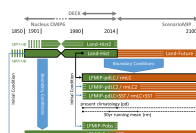


226 *links also exist to C4MIP (terrestrial carbon cycle). Furthermore, a land albedo testbed*
227 *experiment is planned within GeoMIP. From Seneviratne et al. (2014)*

228

229 **Experimental design**

230 The experimental design of LS3MIP consists of a series of offline land-only experiments
231 (LMIP) driven by a land surface forcing data set and a variety of coupled model simulations
232 (LFMIP) (see Figure 4 and Table 1):



233

234 *Figure 4: Schematic diagram for the experiment structure of LS3MIP. Tier 1 experiments are*
235 *indicated with a heavy black outline, and complementary ensemble experiments are*
236 *indicated with white hatched lines. For details on the experiments and acronyms, see Table 1*
237 *and text.*

238

239 (1) Offline land model experiments (“Land offline MIP”, experiment ID “Land”):

240 Offline simulations of land surface states and fluxes allow for the evaluation of trends and
241 variability of snow, soil moisture and land surface fluxes, carbon stocks and vegetation
242 dynamics, and climate change impacts. Within the CMIP6 program various Model
243 Intercomparison Projects make use of offline terrestrial simulations to benchmark or force
244 coupled climate model simulations: LUMIP focusing on the role of land use/land cover
245 change, C4MIP to address the terrestrial component of the carbon cycle and its feedback to
246 climate, and LS3MIP to provide soil moisture and snow boundary conditions.

247 Meteorological forcings, ancillary data (e.g., land use/cover changes, surface parameters,
248 CO₂ concentration and nitrogen deposition) and documented protocols to spin-up and
249 execute the experiments are essential ingredients for a successful offline land model
250 experiment (Wei et al. 2014). The first Global Soil Wetness Project (GSWP; Dirmeyer et al.
251 1999), covering two annual cycles (1987 – 1988), established a successful template, which
252 was updated and fine-tuned in a number of follow-up experiments, both with global
253 (Dirmeyer et al. 2006; Sheffield et al. 2006) and regional (Boone et al. 2009) coverage.

254

255 *Available data sets for meteorological forcing*

256 Offline experiments will primarily use GSWP3³ (Tier 1) forcing (Kim et al., in preparation)
257 with alternate forcing used in Tier 2 experiments.

258 The third Global Soil Wetness Project (GSWP3) provides meteorological forcings for the
259 entire 20th century and beyond, making extensive use of the 20th Century Reanalysis (20CR)

³ <http://hydro.iis.u-tokyo.ac.jp/GSWP3/>



260 (Compo et al. 2011). In this reanalysis product only surface pressure and monthly sea-
261 surface temperature and sea-ice concentration are assimilated. The ensemble uncertainty in
262 the synoptic variability of 20CR varies with the time-changing observation network. High
263 correlations for geopotential height (500 hPa) and air temperature (850 hPa) with an
264 independent long record (1905-2006) of upper-air data were found (Compo et al. 2011),
265 comparable to forecast skill of a state-of-the-art forecasting system at 3 days lead time.

266 GSWP3 forcing data are generated based on a dynamical downscaling of 20CR. A simulation
267 of the Global Spectral Model (GSM), run at a T248 resolution (~50km) is nudged to the
268 vertical structures of 20CR zonal and meridional winds and air temperature using a spectral
269 nudging dynamical downscaling technique that effectively retains synoptic features in the
270 higher spatial resolution (Yoshimura and Kanamitsu 2008). Additional bias corrections using
271 observations, vertical damping (Hong and Chang 2012) and single ensemble member
272 correction (Yoshimura and Kanamitsu 2013) are applied, giving considerable improvements.

273 Weedon et al. (2011) provide the meteorological forcing data for the EU Water and Global
274 Change (WATCH) programme⁴, designed to evaluate global hydrological trends and impacts
275 using offline modelling. The half-degree resolution, 3 hourly WATCH Forcing Data (WFD)
276 was based on the ECMWF ERA-40 reanalysis and included elevation correction and monthly
277 bias correction using CRU observations (and alternative GPCC precipitation total
278 observations). WATCH hydrological modelling led to the WaterMIP study (Haddeland et al.
279 2011). The WFD stops in 2001, but within a follow-up project EMBRACE Weedon et al.
280 (2014) generated the WFDEI dataset that starts in 1979 and was recently extended to 2014.
281 The WFDEI was based on the WATCH Forcing Data methodology but used the ERA-Interim
282 reanalysis (4D-var and higher spatial resolution than ERA-40) so that there are offsets for
283 some variable in the overlap period with the WFD. The forcing consists of 3-hourly ECMWF
284 ERA-Interim reanalysis data (WFD used ERA-40) interpolated to half degree spatial
285 resolution. The 2m temperatures are bias-corrected in terms of monthly means and
286 monthly average diurnal temperature range using CRU half degree observations. The 2m
287 temperature, surface pressure, specific humidity and downwards long-wave radiation fluxes
288 are sequentially elevation corrected. Short-wave radiation fluxes are corrected using CRU
289 cloud cover observations and corrected for the effects of seasonal and interannual changes
290 in aerosol loading. Rainfall and snowfall rates are corrected using CRU wet days per month
291 and according to CRU or GPCC observed monthly precipitation gauge totals. The WFDEI data
292 set is also used as forcing to the ISIMIP2.1 project, which focuses on historical validation of
293 global water balance under transient land use change (Warszawski et al. 2014).

294 To support the Global Carbon Project⁵ (Le Quere et al. 2009) with annual updates of global
295 carbon pools and fluxes, the offline modelling framework TRENDY⁶ applies an ensemble of
296 terrestrial carbon allocation and land surface models. For this a forcing data set is prepared
297 in which NCEP reanalysis data are bias corrected using the gridded in situ climate data from

⁴ <http://www.eu-watch.org/>

⁵ <http://www.globalcarbonproject.org/about/index.htm>

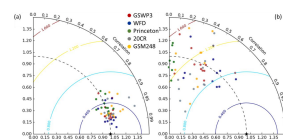
⁶ <http://dgvn.ceh.ac.uk/node/21>



298 the Climate Research Unit (CRU), the so-called CRU-NCEP dataset⁷. This dataset is currently
299 available from 1901 to 2014 at 0.5 degrees horizontal spatial resolution and 6 hourly time-
300 step. It is being updated annually.

301 The Princeton Global Forcing dataset⁸ (Sheffield et al. 2006) was developed as a forcing for
302 land surface and other terrestrial models, and for analyzing changes in near surface climate.
303 The dataset is based on 6-hourly surface climate from the NCEP-NCAR reanalysis, which is
304 corrected for biases at diurnal, daily and monthly time scales using a variety of
305 observational datasets. The data are available at 1.0, 0.5 and 0.25-degree resolution and 3-
306 hourly time-step. The latest version (V2.2) covers 1901-2014, with a real-time extension
307 based on satellite precipitation and weather model analysis fields. The reanalysis
308 precipitation is corrected by adjusting the number of rain days and monthly accumulations
309 to match observations from CRU and the Global Precipitation Climatology Project (GPCP).
310 Precipitation is downscaled in space using statistical relationships based on GPCP and the
311 TRMM Multi-satellite Precipitation Analysis (TMPA), and to 3-hourly resolution based on
312 TMPA. Temperature, humidity, pressure and longwave radiation are downscaled in space
313 with account for elevation. Daily mean temperature and diurnal temperature range are
314 adjusted to match the CRU monthly data. Short- and long-wave surface radiation are
315 adjusted to match satellite-based observations from the University of Maryland (Zhang et al.
316 submitted) and to be consistent with CRU cloud cover observations outside of the satellite
317 period. An experimental version (V3) assimilates station observations into the background
318 gridded field to provide local-scale corrections (Sheffield et al., in preparation).

319 Figure 5 shows the performance in terms of correlation and standard deviation of the
320 forcing data sets compared to daily observations from 20 globally distributed in-situ
321 FLUXNET sites (Baldocchi et al. 2001). Although for precipitation intrinsic heterogeneity
322 leads to significant differences with the in-situ observations, long- and short-wave
323 downward radiation and air temperature show variability characteristics similar to the
324 observations.



325
326 *Figure 5: Taylor diagram for evaluating the forcing datasets comparing to daily observations*
327 *from FLUXNET sites: (a) 2m air temperature and (b) precipitation. Red, blue, and green dots*
328 *indicate GSWP3, Watch Forcing Data (Weedon et al. 2011) and Princeton forcing (Sheffield*
329 *et al. 2006), respectively. Grey and orange dots indicate 20CR and its dynamically*
330 *downscaled product (GSM248).*

331

⁷ Viovy N, Ciais P (2009) A combined dataset for ecosystem modelling, Available at:
<http://dods.extra.cea.fr/data/p529viovy/cruncep/readme.htm>

⁸ <http://hydrology.princeton.edu/data.php>



332 The participating modelling groups are invited to run a number of experiments in this land-
333 only branch of LS3MIP.

334

335 *Historical offline simulations: Land-Hist*

336 The Tier 1 experiments of the offline LMIP experiment consist of simulations using the
337 GSWP3 forcing data for a historical (1831-2014) interval. The land model configuration
338 should be identical to that used in the DECK and CMIP6 historical simulations for the parent
339 coupled model.

340 The atmospheric forcing will be prepared at a standard $0.5 \times 0.5^\circ$ spatial resolution at 3
341 hourly intervals and distributed with a package to regrid data to the native grids of the
342 GCMs. Also vegetation, soil, topography and land/sea mask data will be prescribed
343 following the protocol used for the CMIP6 DECK simulations. Spin-up of the land-only
344 simulations should follow the TRENDY protocol⁹ which calls for recycling of the climate
345 mean and variability from two decades of the forcing dataset (e.g., 1831-1850 for GSWP3,
346 1901-1920 for the alternative land surface forcings). Land use should be held constant at
347 1850 as in the DECK 1850 coupled control simulation (*piControl*). See discussion and
348 definition of “constant land-use” in Section 2.1 of LUMIP protocol paper (Lawrence et al.
349 submitted). CO₂ and all other forcings should be held constant at 1850 levels during spinup.
350 For the period 1850 to the first year of the forcing dataset, the forcing data should continue
351 to be recycled but all other forcings (land-use, CO₂, etc.) should be as in the CMIP6
352 historical simulation. Transient land use is a prescribed CMIP6 forcing and is described in
353 the LUMIP protocol (Lawrence et al. submitted).

354 Single site time series of in-situ observational forcing variables from selected reference
355 locations (from FLUXNET, Baldocchi et al. 2001) are supplied in addition to the forcing data
356 for additional site level validation.

357 Although Land-Hist is not a formal component of the DECK simulations which form the core
358 of CMIP6 (see Fig 2), the WCRP Working Group on Climate Modelling (WGCM) recognized
359 the importance of these land-only experiments for the process of model development and
360 benchmarking. A future implementation of a full or subset of this historical run is proposed
361 to become part of the DECK in future CMIP exercises and is included as a Tier 1 experiment
362 in LS3MIP. Land surface model output from this subset of LMIP will also be used as
363 boundary condition in some of the coupled climate model simulations, described below.

364

365 *Historical simulations with alternative forcings*

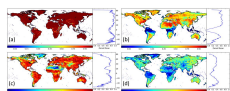
366 Additional Tier 2 experiments are solicited where the experimental set-up is similar to the
367 Tier 1 simulations, but using 3 alternative meteorological forcing data sets that differ from
368 GSWP3: the Princeton forcing (Sheffield et al. 2006), WFD and WFDEI combined (allowing
369 for offsets as needed (Weedon et al. 2014) and the CRU-NCEP forcing (Wei et al. 2014) used
370 in TRENDY (Sitch et al. 2015). These Tier 2 experiments cover the period 1901 – 2014. The

⁹ <http://dgvn.ceh.ac.uk/node/9>



371 model outputs will allow assessment of the sensitivity of land-only simulations to
372 uncertainties in forcing data. Differences in the outputs compared to the primary runs with
373 GSWP3 will help in understanding simulation sensitivity to the selection of forcing datasets.
374 Kim (2010) utilized a similarity index (Ω ; Koster et al. 2000) to estimate the uncertainty
375 derived from an ensemble of precipitation observation data sets relative to the the
376 uncertainty from an ensemble of model simulations for evapotranspiration and runoff. The
377 joint utilization of common monthly observations by the various forcing data sets leads to a
378 high value of Ω when evaluated using monthly mean values. However, evaluation of dataset
379 consistency of monthly variance leads to much larger disparities and considerably lower
380 values of Ω (Figure 6). This uncertainty will propagate differently to other hydrological
381 variables, such as runoff or evapotranspiration (Kim 2010).

382



383

384 *Figure 6: Global distributions of the similarity index (Ω) for 2001-2010 of monthly mean (a, c)*
385 *and (b, d) monthly variance (calculated from daily data from each data set) of 2m air*
386 *temperature (top panels) and precipitation (bottom panels), respectively. Shown are global*
387 *distributions and zonal means. After (Kim 2010).*

388

389 *Climate change impact assessment: Land-Future*

390 A set of future land-only time slice simulations (2015-2100) will be generated via forcing
391 data obtained from at least 2 future climate scenarios from the ScenarioMIP (tentatively,
392 Shared Socio-economic Pathway SSP5-8.5 and SSP4-3.7¹⁰) by 3 model realizations each. The
393 models will be chosen based on the evaluation of the results from the Historical simulations
394 from the CMIP6 Nucleus in order to represent the ensemble spread efficiently and reliably.
395 To generate a set of ensemble forcing data for the future, a trend preserving statistical bias
396 correction method will be applied to the 3-hourly surface meteorology variables (Table A4)
397 from the scenario output (Hempel et al. 2013; Watanabe et al. 2014). Gridded forcings will
398 be provided in a similar data format as the historical simulations.

399 Land-Future is a Tier 2 experiment in LS3MIP and focuses on assessment of climate change
400 impact (e.g. shifts of the occurrence of critical water availability due to changing statistical
401 distributions of extreme events) and on the assessment of the land surface analogue of
402 climate sensitivity for various key land variables (Perket et al. 2014; Flanner et al. 2011).

403

404 (2) Prescribed land surface states in coupled models for land surface feedback assessment 405 (“Land Feedback MIP”, LFMIP):

406 Land surface processes do not act in isolation in the climate system. A tight coupling with
407 the overlying atmosphere takes place on multiple temporal and spatial scales. A systematic

¹⁰ <https://cmip.ucar.edu/scenario-mip/experimental-protocols>



408 assessment of the strength and spatial structure of land surface interaction at
409 subcontinental, seasonal time scales has been performed with the initial GLACE set-up
410 (GLACE1 and GLACE2 experiments; Koster et al. (2004)) in which essentially the spread in an
411 ensemble simulation of a coupled land-atmosphere model was compared to a model
412 configuration in which the land-atmosphere interaction was greatly bypassed by prescribing
413 soil conditions throughout the simulation in all members of the ensemble. Examination of
414 the significance of land-atmosphere feedbacks at the centennial climate time scale was later
415 explored at the regional scale in a single-model study (Seneviratne et al. 2006) and on global
416 scale in the GLACE-CMIP5 experiment in a small model ensemble (Seneviratne et al. 2013).

417 A protocol very similar to the design of GLACE-CMIP5 is followed in LFMIP. Parallel to a set
418 of reference simulations taken from the CMIP6 DECK, a set of forced experiments is carried
419 out where land surface states are prescribed from or nudged towards prescribed fields
420 derived from coupled simulations. The land surface states are prescribed or nudged at a
421 daily time scale.

422 While earlier experiments used model configurations with prescribed SST and sea ice
423 conditions, the Tier 1 experiment in LFMIP will be based on coupled AOGCM simulations
424 and comprise simulations for a historical (1980-2014) and future (2015-2100) time range.
425 The selection of the future scenario (from the ScenarioMIP experiment) will be based on the
426 choices made in the offline LMIP experiment (see above).

427 In GLACE-CMIP5 only soil moisture states were prescribed in the forced experiments. The
428 configuration of the particular land surface models may introduce the need to make
429 different selections of land surface states to be prescribed, for instance to avoid strong
430 inconsistencies in the case of frozen ground (soil moisture rather than soil water state
431 should be prescribed; *M. Hauser, ETH Zurich, personal communication*), melting snow, or
432 growing vegetation. A standardization of this selection is difficult as the implementation and
433 consequences may be highly model specific. Here we recommend to prescribe only the
434 water reservoirs (soil moisture, snow mass). The disparity of possible implementations is
435 adding to the uncertainty range generated by the model ensemble, similar to the degree to
436 which implementation of land use, flux corrections or downscaling adds to this uncertainty
437 range. Participating modelling groups are encouraged to apply various test simulations
438 focusing both on technical feasibility and experimental impact to evaluate different
439 procedures to prescribe land surface conditions.

440 The earlier experience with GLACE-type experiments has revealed a number of technical
441 and scientific issues. Because in most GCMs the land surface module is an integral part of
442 the code describing the atmosphere, prescribing land surface dynamics requires a non-
443 conventional technical interface, reading and replacing variables throughout the entire
444 simulations. Many participants to LS3MIP have participated earlier in GLACE-type
445 experiments, but for some the code adjustments will require a technical effort.
446 Interpretation of the effect of the variety of implementations of prescribed land surface
447 variables by the different modelling groups (see above) is helped by a careful
448 documentation of the way the modelling groups have implemented this interface. Tight
449 coordination and frequent exchange among the participating modelling groups on the



450 technical modalities of the implementation of the required forcing methods will be ensured
451 during the preparatory phase of LS3MIP in order to maximize the coherence of the
452 modelling exercise and to facilitate the interpretation of the results.

453 By design, the prescribed land surface experiments do not fully conserve water and energy,
454 similar to AMIP, nudged, and data assimilation experiments. A systematic addition or
455 removal of water or energy can even emerge as a result of asymmetric land surface
456 responses to dry and to wet conditions, e.g. when surface evaporation or runoff depend
457 strongly non-linearly to soil moisture or snow states (e.g. Jaeger and Seneviratne 2011).
458 Also, unrepresented processes (such as water extraction for irrigation or exchange with the
459 groundwater) may lead to imbalances in the budget (Wada et al. 2012). This systematic
460 alteration of the water and energy balance may not only perturb the simulation of present-
461 day climate (e.g. Douville 2003; Douville et al. 2016) but may also interact with the
462 projected climate change signal, where altered climatological soil conditions can contribute
463 to the climate change induced temperature or precipitation signal or water imbalances can
464 lead to imposed runoff changes that could affect ocean circulation and SSTs. Earlier GLACE-
465 type experiments revealed that the problems of water conservation are often reduced when
466 prescribed soil water conditions are taken as the median rather than the mean of a sample
467 over which a climatological mean is calculated (Hauser et al. *subm*). In the analyses of the
468 experiments this asymmetry and lack of energy/water balance closure will be examined and
469 put in context of the climatological energy and water balance and its climatic trends.

470 To be able to best quantify the forcing that prescribing the land surface state represents,
471 the increments of both snow and soil moisture imposed as a consequence of this
472 prescription are required as an additional output. This will enable us to estimate the
473 amplitude of implicit water and energy fluxes imposed by the forcing procedure.

474 Complementary experiments following an almost identical setup as LFMIP, but limiting the
475 prescription of land surface variables to snow-related variables and thus leaving soil
476 moisture free-running, are carried out in the framework of the ESM-SnowMIP (Earth System
477 Model - Snow Module Intercomparison Project) carried out within the WCRP Grand
478 Challenge “Melting Ice and Global Consequences”¹¹. ESM-SnowMIP being tightly linked to
479 LS3MIP, these complementary experiments will allow separating effects of soil moisture and
480 snow feedbacks.

481

482 *Tier 1 experiments in LFMIP*

483 Similar to the set-up of GLACE-CMIP5 (Seneviratne et al. 2013), the core experiments of
484 LFMIP (tier 1) evaluate two different sets of prescribed land surface conditions (snow and
485 soil moisture):

- 486 • LFMIP-pdLC: the experiments comprise transient coupled atmosphere-ocean
487 simulations in which a selection of land surface characteristics is prescribed rather
488 than interactively calculated in the model. This “climatological” land surface forcing

¹¹ <http://www.climate-cryosphere.org/activities/targeted/esm-snowmip>



489 is calculated as the mean annual cycle in the period 1980-2014 from the Historical
 490 GCM simulations. The experiment aims at diagnosing the role of land-atmosphere
 491 feedback at the climate time scale. Seneviratne et al. (2013) found a substantial
 492 effect of changes in climatological soil moisture on projected temperature change in
 493 a future climate, both for seasonal mean and daytime extreme temperature in
 494 summer. Effects on precipitation are less clear, and the multi-model nature of
 495 LS3MIP is designed to sharpen these quantitative effects. Also, LS3MIP will take a
 496 potential damping (or amplifying) effect of oceanic responses on altered land surface
 497 conditions into account, in contrast to GLACE-CMIP5. Experiments using this set-up
 498 (i.e. coupled ocean) in a single-model study have shown that the results could be
 499 slightly affected by the inclusion of an interactive ocean, although the effects were
 500 not found to be large overall (Orth and Seneviratne submitted).

- 501 • LFMIP-rmLC: a prescribed climatology using a transient 30-yr running mean, where a
 502 comparison to the standard CMIP6 runs allows diagnosis of shifts in the regions of
 503 strong land-atmosphere coupling as recorded by e.g. Seneviratne et al. (2006), and
 504 shifts in potential predictability related to land surface states (Dirmeyer et al. 2013).

505 Both sets of simulations cover the historical period (1850-2014) and extend to 2100, based
 506 on a forcing scenario to be identified at a later stage.

507 Output in high temporal resolution (daily, as well as sub-daily for some fields and time
 508 slices) is required to address the role of land surface-climate feedbacks on climate extremes
 509 over land.

510 Multi-member experiments are encouraged, but the mandatory tier 1 simulations are
 511 limited to one realization for each of the two prescribed land surface time series described
 512 above.

513

514 *Tier 2 experiments in LFMIP*

515 To analyse a number of additional features of land-atmosphere feedbacks, a collection of
 516 tier 2 simulations is proposed in LS3MIP:

- 517 • *Simulations with observed SST*: The AOGCM simulations from Tier 1 are duplicated
 518 with a prescribed SST configuration taken from the AMIP runs in the DECK (AGCM),
 519 in order to isolate the role of the ocean in propagating and damping/reinforcing land
 520 surface responses on climate (Koster et al. 2000). Both the historic and running
 521 mean land surface simulations are requested (LFMIP-pdLC+SST and -rmLC+SST,
 522 respectively)
- 523 • *Simulations with observed SST and Land-hist output*: A “perfect boundary condition”
 524 set of experiments use the AMIP SSTs and the Land-Hist land boundary conditions
 525 generated by the land surface model used in the participating ESM, leading to
 526 simulations driven by surface fields that are strongly controlled by observed forcings.
 527 This will only cover the historic period (1901-2014) (LFMIP-PObs+SST). For this the
 528 land-only simulations in LMIP need to be interpolated to the native GCM grid,
 529 preserving land-sea boundaries and other characteristics.



- 530 • *Separate effects of soil moisture and snow, and role of additional land parameters*
531 *and variables*: Additional experiments, in which only snow, snow albedo or soil
532 moisture is prescribed will be conducted to assess the respective feedbacks in
533 isolation, and have control on possible interactions between snow cover and soil
534 moisture content. Also vegetation parameters and variables (e.g. leaf area index,
535 canopy height and thickness) are considered. These experiments are not listed in
536 Table 1, but will be detailed in a follow-up protocol to be defined later.
- 537 • *Fixed land use conditions*: in conjunction with the Land Use MIP (LUMIP) a repetition
538 of the Tier 1 experiment under fixed 1850 land cover and land use conditions
539 highlights the role of soil moisture in modulating the climate response to land cover
540 and land use. (Not listed in Table 1)

541

542 (3) Prescribed land surface states derived from pseudo-observations (LFMIP-Pobs)

543 The use of LMIP (land-only simulations) to initialize the AOGCM experiments (LFMIP) allows
544 a set of predictability experiments in line with the GLACE2 set-up (Koster et al. 2010a). The
545 LFMIP-Pobs experiment is an extension to GLACE2 by (a) allowing more models to
546 participate, (b) improving the statistics by extending the original 1986 – 1995 record to 1980
547 – 2014, (c) evaluating the quality of newly available land surface forcings, and (d) executing
548 the experiments in AOGCM mode. Koster et al. (2010a) and van den Hurk et al. (2012)
549 concluded that the forecast skill improvement from models using initial soil moisture
550 conditions was relatively low. Possible causes for this low skill are the limited record length
551 and limited quality of the (precipitation) observations used to generate the soil conditions.
552 These issues are explicitly addressed in LFMIP-Pobs.

553 All LFMIP-Pobs experiments are Tier 2, which also gives room for additional model design
554 elements such as the evaluation of various observational data sources (such as for SWE or
555 snow albedo, using satellites derived, reanalysis and land surface model outputs). The
556 predictability assessments include the evaluation of the contribution of snow cover melting
557 and its related feedbacks to the underestimation of recent boreal polar warming by climate
558 models.

559 The experimental protocol (number of simulations years, ensemble size, initialization, model
560 configuration, output diagnostics) has a strong impact on the results of the experiment (e.g.
561 Guo and Dirmeyer 2013). This careful design of the LFMIP-Pobs experiment needed for a
562 succesfull implementation has currently not yet taken place. Therefore these experiments
563 are listed as Tier 2 in Table 1, with the comment that the detailed experimental protocol still
564 needs to be defined.

565



566 *Table 1: Summary of LS3MIP experiments. Experiments with specific treatment of subsets of*
 567 *land surface features are not listed in this overview.*

Experiment ID and Tier	Experiment Description / Design	Config (L/A/O)*	Start	End	# Ens**	# Total Years***	Science Question and/or Gap Being Addressed	Synergies with other CMIP6 MIPs
Land-Hist (1)	Land only simulations	L	1850	2014	1	165	Historical land simulations	LUMIP, C4MIP, CMIP6 historical
Land-Hist2 (2)	Land only simulations	L	1901	2014	3	342	As Land-Hist but with three different forcing data sets (Princeton forcing, CRU-NCEP, and WFDEI)	
Land-Future (2)	Land only simulations	L	2015	2100	6	516	Climate trend analysis	LUMIP, C4MIP, ScenarioMIP
LFMIP-pdLC (1)	Prescribed land conditions 1980-2014 climate	LAO	1980	2100	1	121	diagnose land-climate feedback including ocean response	ScenarioMIP
LFMIP-pdLC2 (2)	as LFMIP-pdLC with multiple model members	LAO	1980	2100	4	484	diagnose land-climate feedback including ocean response	ScenarioMIP
LFMIP-pdLC+SST (2)	Prescribed land conditions 1980-2014 climate; SSTs prescribed	LA	1980	2100	5	605	diagnose land-climate feedback over land	ScenarioMIP
LFMIP-Pobs+SST (2)	Land conditions from Land-hist; SSTs prescribed	LA	1901	2014	1	115	“perfect boundary condition” simulations	
LFMIP-rmLC (1)	Prescribed land conditions 30yr running mean	LAO	1980	2100	1	121	diagnose land-climate feedback including ocean response	ScenarioMIP
LFMIP-rmLC2 (2)	as LFMIP-rmLC with multiple model members	LAO	1980	2100	4	484	diagnose land-climate feedback including ocean response	ScenarioMIP
LFMIP-rmLC+SST (2)	Prescribed land conditions 30yr running mean; SSTs prescribed	LA	1980	2100	5	605	diagnose land-climate feedback over land	ScenarioMIP
LFMIP-Pobs (2) ^{ptbd}	Initialized pseudo-observations land	LAO	1980	2014	10	350	land-related seasonal predictability	CMIP6 historical

568 *Config L/A/O refers to land/atmosphere/ocean model configurations

569 ** # Ens refers to number of ensemble members.

570 *** # Total years is total number of simulation years.

571 ^{ptbd} experimental protocol needs to be detailed in a later stage



572

573 **Analysis strategy**

574 LS3MIP is designed to push the land surface component of climate models, observational
575 data sets and projections to a higher level of maturity. Understanding the propagation of
576 model and forecast errors and the design of model parameterizations is essential to realize
577 this goal. The LS3MIP steering group is a multi-disciplinary team (climate modellers, snow
578 and soil moisture model specialists, experts in local and remotely sensed data of soil
579 moisture and snow properties) that ensures that the experiment setups, model evaluations
580 and analyses/interpretations of the results are pertinent.

581 For both snow and soil moisture the starting point will be a careful analysis of model results
582 from on the one hand a) the DECK historic simulations (both the AMIP and the historical
583 coupled simulation) and b) on the other hand the (offline) LMIP historical simulations.

584 For the evaluation of snow representation in the models, large-scale high-quality datasets of
585 snow mass (SWE) and snow cover extent (SCE) with quantitative uncertainty characteristics
586 will be provided by the Satellite Snow Product Intercomparison and Evaluation Experiment
587 (SnowPEX¹²). Analysis within SnowPEX is providing the first evaluation of satellite derived
588 snow extent (15 participating datasets) and SWE derived from satellite measurements, land
589 surface assimilation systems, physical snow models, and reanalyses (7 participating
590 datasets). Internal consistency between products, and bias relative to independent
591 reference datasets are being derived based on standardized and consistent protocols. The
592 evaluation of variability and trends in terrestrial snow cover extent and mass was examined
593 previously for CMIP3 and CMIP5 by e.g. Brown and Mote (2009), Derksen and Brown (2012)
594 and Brutel-Vuilmet et al. (2013). While these assessments were based on single
595 observational datasets, and hence provide no perspective on observational uncertainty and
596 spread relative to multi-model ensembles, standardized multi-source datasets generated by
597 SnowPEX will allow assessment using a multi-dataset observational ensemble (e.g. Mudryk
598 et al. 2015). For snow albedo, multiple satellite-derived datasets are available, including 16-
599 day MODIS¹³ data from 2001 – present, the ESA GlobAlbedo product¹⁴, the recently updated
600 twice-daily APP-x¹⁵ product (1982 – 2011), and a derivation of the snow shortwave radiative
601 effect from 2001 – 2013 (Singh et al. 2015). Satellite retrievals of snow cover fraction in
602 forested and mountainous areas is an ongoing area of uncertainty which influences the
603 essential diagnostics related to climate sensitivity of snow cover (Thackeray et al. 2015b),
604 feeding into essential diagnostics related to climate sensitivity of snow cover (Qu and Hall,
605 2014; Fletcher et al. 2012).

¹² <http://calvalportal.ceos.org/projects/snowpex>

¹³ <http://modis-atmos.gsfc.nasa.gov/ALBEDO/>

¹⁴ <http://www.globalbedo.org>

¹⁵ <http://stratus.ssec.wisc.edu/products/appx/appx.html>



606 In the case of soil moisture, land hydrology and vegetation state, several observations-based
607 datasets will be used in the evaluation of the coupled DECK simulations and offline Land
608 experiments. Data considered will include the first multidecadal satellite-based global soil
609 moisture record (Essential Climate Variable Soil Moisture ECVSM) (Liu et al. 2012; Dorigo et
610 al. 2012), long-term (2002-2015) records of terrestrial water storage from the GRACE
611 satellite (Rodell et al. 2009; Reager et al. 2016; Kim et al. 2009), the multi-product LandFlux-
612 EVAL evapotranspiration synthesis (Mueller et al. 2013), multi-decadal satellite retrievals of
613 the Fraction of Photosynthetically Absorbed Radiation (FPAR, e.g. Gobron et al. 2010;
614 Zscheischler et al. 2015), and upscaled Fluxnet based products (Jung et al. 2010).

615 Several details of snow and soil moisture dynamical processes can be indirectly inferred
616 through the analysis of river discharge (Orth et al. 2013; Zampieri et al. 2015). Variables
617 simulated by the routing schemes included in the land surface models can be compared
618 with the station data available from the Global Runoff Database (GRDC¹⁶). Combined use of
619 in-situ discharge observations and terrestrial water storage changes observed by GRACE will
620 verify how the land surface simulations partition the terms in the water balance equation
621 (i.e., precipitation, evapotranspiration, runoff, and water storage changes)(Kim et al. 2009).

622 The coupled LS3MIP (LFMIP) simulations will be analyzed in concert with the control runs to
623 quantify various climatic effects of snow and soil moisture, detect systematic biases and
624 diagnose feedbacks. Anticipated analyses include:

- 625 • *Drivers of variability at multiple time scales:* comparison of simulations with
626 prescribed soil moisture and snow (LFMIP-pdLC) allows the quantification of the
627 impact of land surface state variability on variability of climate variables as, for
628 instance, temperature, relative humidity, cloudiness, precipitation and river
629 discharge at several time scale. The LFMIP-rmLC simulation allows evaluation of this
630 contribution on seasonal time scales, and changes of patterns of high/low land
631 surface impact in a future climate. In particular, a focus will be set on impacts on
632 climate extremes (temperature extremes, heavy precipitation events, see e.g.
633 Seneviratne et al. 2013) and the possible role of land-based feedbacks in amplifying
634 regional climate responses compared to changes in global mean temperature
635 (Seneviratne et al. 2016). A secondary focus will be on the impacts of snow and soil
636 moisture variability on the extremes of river discharge, which can be related to large-
637 scale floods and to non-local propagation of droughts signal. These aspects will be
638 analyzed in the context of water management and to quantify feedbacks of the river
639 discharge on the climate system (through the discharge in the oceans, Matera et al.
640 2012; Carmack et al. 2015) and to the carbon cycle (through the methane produced
641 in flooded areas, Meng et al. 2015)).
- 642 • *Attribution of model disagreement:* the multi-model set up of the experiment allows
643 closer inspection of the effects of modeled soil moisture and snow (and related

¹⁶ <http://www.bafg.de/GRDC>



- 644 processes such as plant transpiration, photosynthesis, or snowmelt) to calculated
645 land temperature, precipitation, runoff, vegetation state, and gross primary
646 production. The comparison of LFMIP-pdLC and LFMIP-rmLC will be useful to isolate
647 the model disagreement in land surface feedbacks potentially induced by including
648 coupling to a dynamic ocean despite similar land response to climate change.
- 649 • *Emergent constraints*: while the annual cycle of snow cover and local temperature
650 (Qu and Hall 2014), and the relation between global mean temperature fluctuations
651 and CO₂-concentration (Cox et al. 2013) provide observational constraints on snow-
652 albedo and carbon-climate feedback respectively, similar emergent constraints may
653 be defined to constrain (regional) soil moisture or snow related feedbacks with
654 temperature or hydrological processes such as, for instance, the timing of spring
655 onset which may be related to snowmelt, spring river discharge (Zampieri et al.
656 2015) and vegetation phenology (Xu et al. 2013). Use of appropriate observations
657 and diagnostics as emergent constraints will reduce uncertainties in projections of
658 mean climate and extremes (heat extremes, droughts, floods) (Hoffman et al. 2014).
659 The analysis of amplitude and timing of seasonality of hydrological and ecosystem
660 processes will provide additional diagnostics.
 - 661 • *Attribution of model bias*: a positive relationship between model temperature bias in
662 the current climate, and (regional) climate response can partly be attributed to the
663 soil moisture-climate feedback, which acts on both the seasonal and climate time
664 scale (Cheruy et al. 2014). A multi-model assessment of this relationship is enabled
665 via LS3MIP. The comparison of AMIP-DECK, LFMIP-CA and LFMIP-LCA will be used to
666 assess the impact of atmospheric-related errors in land boundary conditions on the
667 AGCM biases.
 - 668 • *Changes in feedback hotspots and predictability patterns*: land surface conditions
669 don't exert uniform influence on the atmosphere in all areas of the globe: a
670 distribution of strong interaction "hotspots" and areas of high potential predictability
671 contributions from the land surface exists (e.g. Koster et al. 2004). These patterns
672 may change in a future climate (e.g. Seneviratne et al. 2006). A multi-model
673 assessment such as foreseen in LS3MIP allows mapping changes in these patterns,
674 with implications for the occurrence of droughts, heat waves, irrigation limitations or
675 river discharge anomalies and their predictability (Dirmeyer et al. 2013).
 - 676 • *Snow shortwave radiative effect analysis*: The Snow Shortwave Radiative Effect
677 (SSRE) can be diagnosed through parallel calculations of surface albedo and
678 shortwave fluxes with and without model snow on the ground or in the vegetation
679 canopy (Perket et al. 2014). This metric provides a precise, overarching measure of
680 the snow-induced perturbation to solar absorption in each model, integrating over
681 the variable influences of vegetation masking, snow grain size, snow cover fraction,
682 soot content, etc. SSRE is analogous to the widely-used cloud radiative effect
683 diagnostic, and its time evolution provides a measure of snow albedo feedback in



684 the context of changing climate (Flanner et al. 2011). We recommend that the
 685 diagnostic snow shortwave radiative effect (SSRE) calculation be implemented in
 686 standard LS3MIP simulations (Tiers 1 and 2). This will enable us to evaluate the
 687 integrated effect of model snow cover on surface radiative fluxes.

- 688 • *Complementary snow-related offline experiments:* Additional offline experiments
 689 with prescribed snow albedo or snow water equivalent are planned as a follow-up to
 690 LS3MIP within the ESM-SnowMIP¹⁷ initiative. This is aimed at improving our
 691 understanding of sources of coupled model biases (global offline and site scale
 692 experiments) in order to identify priority avenues for future model development.

693 Regarding the snow analyses, the initial geographical focus of LS3MIP is on the continental
 694 snow cover of both hemispheres, both in ice-free areas (Northern Eurasia and North
 695 America) and on the large ice sheets (Greenland and Antarctica). Effects of snow on sea ice,
 696 and the quality of the representation of snow on sea ice in climate models, will be explored
 697 later, but is of interest because of strong recent trends of Arctic sea ice decline and the
 698 potential amplifying effect of earlier spring snow melt over land.

699 For soil moisture, the geographical focus is on all land areas, with special interest in
 700 locations with strong land-atmosphere interaction (transition zones between wet and dry
 701 climates), extensive irrigation areas, and high interannual variability of warm season climate
 702 in densely populated areas.

703 The analyses are carried out on a standardized model output data set. A summary of the
 704 requested output data is given in tables in the Annex.

705
 706

Table 2: Earth System Modelling groups participating to LS3MIP

Model Name	Institute	Country
ACCESS	CSIRO/Bureau of Meteorology	Australia
ACME Land Model	U.S. Department of Energy	USA
BCC-CSM2-MR	BCC,CMA	China
CanESM	CCCma	Canada
CESM		USA
CMCC-CM2	Centro Euro-Mediterraneo sui Cambiamenti Climatici	Italy
CNRM-CM	CNRM-CERFACS	France
EC-Earth	SMHI and 26 other institutes	Sweden and 9 other European countries
FGOALS	LASG, IAP, CAS	China

¹⁷ <http://www.climate-cryosphere.org/activities/targeted/esm-snowmip>



GISS	NASA GISS	USA
IPSL-CM6	IPSL	France
MIROC6-CGCM	AORI, University of Tokyo / JAMSTEC / National Institute for Environmental Studies	Japan
MPI-ESM	Max Planck Institute for Meteorology (MPI- M)	Germany
MRI-ESM1.x	Meteorological Research Institute	Japan
NorESM	Norwegian Climate Service Centre	Norway
hadGEM3	Met Office	UK

707

708 **Data availability**

709 The offline forcing data for the Land-Hist experiments and output from the model
 710 simulations described in this paper will be distributed through the Earth System Grid
 711 Federation (ESGF) with digital object identifiers (DOIs) assigned. The model output required
 712 for LS3MIP is listed in the Annex. Model data distributed via ESGF will be freely accessible
 713 through data portals after registration. Links to all forcings datasets will be made available
 714 via the CMIP Panel website¹⁸. Information about accreditation, data infrastructure,
 715 metadata structure, citation and acknowledging is provided by Eyring et al. (2015).

716

717 **Time line and participating models**

718 The offline land surface experiments (Land-Hist) are expected to be completed in early
 719 2017. Future time slices can only be performed when the Scenario-MIP results become
 720 available. All coupled LS3MIP simulations and their subsequent analyses will be timed after
 721 the completion of the DECK and historical 20th century simulations, expected by mid 2017.
 722 Table 2 lists the participating Earth System modelling groups.

723

724 **Discussion: expected outcome and impact of LS3MIP**

725 The treatment of the land surface in the current generation of climate models plays a critical
 726 role in the assessment of potential effects of widespread changes in radiative forcing, land
 727 use and biogeochemical cycles. The land surface both “receives” climatic variations (by its
 728 atmospheric forcing) and “returns” these variations as feedbacks or land surface features
 729 that are of high relevance to the people living on it. The strong coupling between land
 730 surface, atmosphere, hydrosphere and cryosphere makes an analysis of its performance
 731 characteristics challenging: the response and the state of the land surface strongly depend
 732 on the climatological context, and metrics of interactions or feedbacks, which are all difficult
 733 to define and observe (van den Hurk et al. 2011).

734 LS3MIP addresses these challenges by enhancing earlier diagnostic studies and experimental
 735 designs. It will lead to enhanced understanding of the contribution of land surface

¹⁸ <http://www.wcrp-climate.org/index.php/wgcm-cmip/about-cmip>



736 treatment to overall climate model performance; give inspiration on how to optimize land
737 surface parameterizations or its forcing; support the development of better forecasting
738 tools, where initial conditions affect the trajectory of the forecast and can be used to
739 optimize forecast skill; and, last but not least, provide a better historical picture of the
740 evolution of our vital water resources during the recent century. In particular, LS3MIP will
741 provide a solid benchmark for assessing water and climate related risks and trends therein.
742 Given the critical importance of changes in land water availability and of impacts of changes
743 in snow, soil moisture and land surface states for the projected evolution of climate mean
744 and extremes, we expect that LS3MIP will help the research community make fundamental
745 advances in this area.

746

747 **Acknowledgements**

748 The authors thank the CMIP panel of the WCRP Working Group on Climate Modelling for
749 their efforts in coordinating the CMIP6 enterprise. G.P.W. was supported by the Joint UK
750 DECC/Defra Met Office Hadley Climate Centre Programme (GA01101). J.M. is supported by
751 the Biogeochemistry-Climate Feedbacks Scientific Focus Area project funded through the
752 Regional and Global Climate Modeling Program in Climate and Environmental Sciences
753 Division (CESD) of the Biological and Environmental Research (BER) Program in the U.S.
754 Department of Energy Office of Science. Oak Ridge National Laboratory is managed by UT-
755 BATTELLE for under contract DE-AC05-00OR22725. Hanna Lee (NorESM) has expressed
756 intention to participate in LS3MIP when feasible, but has not contributed to this manuscript.

757

758 **References**

- 759 Anav, A., and Coauthors, 2013: Evaluating the Land and Ocean Components of the Global
760 Carbon Cycle in the CMIP5 Earth System Models. *J. Clim.*, **26**, 6801–6843,
761 doi:10.1175/JCLI-D-12-00417.1.
- 762 Baldocchi, D., and Coauthors, 2001: FLUXNET: A New Tool to Study the Temporal and Spatial
763 Variability of Ecosystem-Scale Carbon Dioxide, Water Vapor, and Energy Flux
764 Densities. *Bull. Am. Meteorol. Soc.*, **82**, 2415–2434, doi:10.1175/1520-
765 0477(2001)082<2415:FANTTS>2.3.CO;2.
- 766 Boone, A., and Coauthors, 2009: The AMMA Land Surface Model Intercomparison Project
767 (ALMIP). *Bull. Am. Meteorol. Soc.*, **90**, 1865–1880, doi:10.1175/2009BAMS2786.1.
- 768 Brown, R. D., and P. W. Mote, 2009: The Response of Northern Hemisphere Snow Cover to a
769 Changing Climate*. *J. Clim.*, **22**, 2124–2145, doi:10.1175/2008JCLI2665.1.
- 770 Brutel-Vuilmet, C., M. Ménégoz, and G. Krinner, 2013: An analysis of present and future
771 seasonal Northern Hemisphere land snow cover simulated by CMIP5 coupled climate
772 models. *The Cryosphere*, **7**, 67–80, doi:10.5194/tc-7-67-2013.



- 773 Campoy, A., A. Ducharne, F. Cheruy, F. Hourdin, J. Polcher, and J. C. Dupont, 2013: Response
774 of land surface fluxes and precipitation to different soil bottom hydrological
775 conditions in a general circulation model. *J. Geophys. Res. Atmospheres*, **118**,
776 10,725–10,739, doi:10.1002/jgrd.50627.
- 777 Carmack, E., and Coauthors, 2015: Fresh water and its role in the Arctic Marine System:
778 sources, disposition, storage, export, and physical and biogeochemical consequences
779 in the Arctic and global oceans. *J. Geophys. Res. Biogeosciences*, n/a – n/a,
780 doi:10.1002/2015JG003140.
- 781 Cattiaux, J., H. Douville, and Y. Peings, 2013: European temperatures in CMIP5: origins of
782 present-day biases and future uncertainties. *Clim. Dyn.*, **41**, 2889–2907,
783 doi:10.1007/s00382-013-1731-y.
- 784 Cheruy, F., J. L. Dufresne, F. Hourdin, and A. Ducharne, 2014: Role of clouds and land-
785 atmosphere coupling in midlatitude continental summer warm biases and climate
786 change amplification in CMIP5 simulations. *Geophys. Res. Lett.*, **41**, 6493–6500,
787 doi:10.1002/2014GL061145.
- 788 Clark, M. P., and Coauthors, 2015: Improving the representation of hydrologic processes in
789 Earth System Models. *Water Resour. Res.*, **51**, 5929–5956,
790 doi:10.1002/2015WR017096.
- 791 Compo, G. P., and Coauthors, 2011: The Twentieth Century Reanalysis Project. *Q. J. R.*
792 *Meteorol. Soc.*, **137**, 1–28, doi:10.1002/qj.776.
- 793 Cox, P. M., D. Pearson, B. B. Booth, P. Friedlingstein, C. Huntingford, C. D. Jones, and C. M.
794 Luke, 2013: Sensitivity of tropical carbon to climate change constrained by carbon
795 dioxide variability. *Nature*, **494**, 341–344, doi:10.1038/nature11882.
- 796 Derksen, C., and R. Brown, 2012: Spring snow cover extent reductions in the 2008–2012
797 period exceeding climate model projections. *Geophys. Res. Lett.*, **39**, L19504,
798 doi:10.1029/2012GL053387.
- 799 Dirmeyer, P. A., A. J. Dolman, and N. Sato, 1999: The Pilot Phase of the Global Soil Wetness
800 Project. *Bull. Am. Meteorol. Soc.*, **80**, 851–878, doi:10.1175/1520-
801 0477(1999)080<0851:TPPOTG>2.0.CO;2.
- 802 —, X. Gao, M. Zhao, Z. Guo, T. Oki, and N. Hanasaki, 2006: GSWP-2: Multimodel Analysis
803 and Implications for Our Perception of the Land Surface. *Bull. Am. Meteorol. Soc.*, **87**,
804 1381–1397, doi:10.1175/BAMS-87-10-1381.
- 805 —, S. Kumar, M. J. Fennessy, E. L. Altshuler, T. DelSole, Z. Guo, B. A. Cash, and D. Straus,
806 2013: Model Estimates of Land-Driven Predictability in a Changing Climate from
807 CCSM4. *J. Clim.*, **26**, 8495–8512, doi:10.1175/JCLI-D-13-00029.1.
- 808 Dorigo, W., R. de Jeu, D. Chung, R. Parinussa, Y. Liu, W. Wagner, and D. Fernández-Prieto,
809 2012: Evaluating global trends (1988–2010) in harmonized multi-satellite surface soil
810 moisture. *Geophys. Res. Lett.*, **39**, n/a – n/a, doi:10.1029/2012GL052988.



- 811 Douville, Conil, Tyteca, and Voldoire, 2007: Soil moisture memory and West African
812 monsoon predictability: artefact or reality? *Clim. Dyn.*, **28**, 723–742,
813 doi:10.1007/s00382-006-0207-8.
- 814 Douville, H., 2003: Assessing the Influence of Soil Moisture on Seasonal Climate Variability
815 with AGCMs. *J. Hydrometeorol.*, **4**, 1044–1066, doi:10.1175/1525-
816 7541(2003)004<1044:ATIOSM>2.0.CO;2.
- 817 —, A. Ribes, B. Decharme, R. Alkama, and J. Sheffield, 2013: Anthropogenic influence on
818 multidecadal changes in reconstructed global evapotranspiration. *Nat. Clim Change*,
819 **3**, 59–62, doi:10.1038/nclimate1632.
- 820 —, J. Colin, E. Krug, J. Cattiaux, and S. Thao, 2016: Midlatitude daily summer temperatures
821 reshaped by soil moisture under climate change. *Geophys. Res. Lett.*, **43**, 812–818,
822 doi:10.1002/2015GL066222.
- 823 Essery, R., and Coauthors, 2009: SNOWMIP2: An Evaluation of Forest Snow Process
824 Simulations. *Bull. Am. Meteorol. Soc.*, **90**, 1120–1135,
825 doi:10.1175/2009BAMS2629.1.
- 826 Etchevers, P., and Coauthors, 2004: Validation of the energy budget of an alpine snowpack
827 simulated by several snow models (SnowMIP project). *Ann. Glaciol.*, **38**, 150–158,
828 doi:10.3189/172756404781814825.
- 829 Eyring, V., S. Bony, G. A. Meehl, C. Senior, B. Stevens, R. J. Stouffer, and K. E. Taylor, 2015:
830 Overview of the Coupled Model Intercomparison Project Phase 6 (CMIP6)
831 experimental design and organisation. *Geosci Model Dev Discuss*, **2015**, 10539–
832 10583, doi:10.5194/gmdd-8-10539-2015.
- 833 Flanner, M. G., K. M. Shell, M. Barlage, D. K. Perovich, and M. A. Tschudi, 2011: Radiative
834 forcing and albedo feedback from the Northern Hemisphere cryosphere between
835 1979 and 2008. *Nat. Geosci.*, **4**, 151–155, doi:10.1038/ngeo1062.
- 836 Fletcher, C. G., S. C. Hardiman, P. J. Kushner, and J. Cohen, 2009: The Dynamical Response to
837 Snow Cover Perturbations in a Large Ensemble of Atmospheric GCM Integrations. *J.*
838 *Clim.*, **22**, 1208–1222, doi:10.1175/2008JCLI2505.1.
- 839 —, H. Zhao, P. J. Kushner, and R. Fernandes, 2012: Using models and satellite observations
840 to evaluate the strength of snow albedo feedback. *J. Geophys. Res. Atmospheres*,
841 **117**, D11117, doi:10.1029/2012JD017724.
- 842 Friedlingstein, P., M. Meinshausen, V. K. Arora, C. D. Jones, A. Anav, S. K. Liddicoat, and R.
843 Knutti, 2013: Uncertainties in CMIP5 Climate Projections due to Carbon Cycle
844 Feedbacks. *J. Clim.*, **27**, 511–526, doi:10.1175/JCLI-D-12-00579.1.
- 845 Gobron, N., A. Belward, B. Pinty, and W. Knorr, 2010: Monitoring biosphere vegetation
846 1998–2009. *Geophys. Res. Lett.*, **37**, n/a – n/a, doi:10.1029/2010GL043870.



- 847 Gouttevin, I., M. Menegoz, F. Dominé, G. Krinner, C. Koven, P. Ciais, C. Tarnocai, and J.
848 Boike, 2012: How the insulating properties of snow affect soil carbon distribution in
849 the continental pan-Arctic area. *J. Geophys. Res. Biogeosciences*, **117**, n/a – n/a,
850 doi:10.1029/2011JG001916.
- 851 Greve, P., B. Orlowsky, B. Mueller, J. Sheffield, M. Reichstein, and S. I. Seneviratne, 2014:
852 Global assessment of trends in wetting and drying over land. *Nat. Geosci*, **7**, 716–
853 721.
- 854 Guo, Z., and P. A. Dirmeyer, 2013: Interannual Variability of Land–Atmosphere Coupling
855 Strength. *J. Hydrometeorol.*, **14**, 1636–1646, doi:10.1175/JHM-D-12-0171.1.
- 856 Haddeland, I., and Coauthors, 2011: Multimodel Estimate of the Global Terrestrial Water
857 Balance: Setup and First Results. *J. Hydrometeorol.*, **12**, 869–884,
858 doi:10.1175/2011JHM1324.1.
- 859 Hall, A., X. Qu, and J. D. Neelin, 2008: Improving predictions of summer climate change in
860 the United States. *Geophys. Res. Lett.*, **35**, L01702, doi:10.1029/2007GL032012.
- 861 Hauser, M., R. Orth, and S. I. Seneviratne, subm: Role of soil moisture vs recent climate
862 change for heat waves in western Russia. *Geophys.Res.Lett.*,.
- 863 Hempel, S., K. Frieler, L. Warszawski, J. Schewe, and F. Piontek, 2013: A trend-preserving
864 bias correction – the ISI-MIP approach. *Earth Syst Dynam*, **4**, 219–236,
865 doi:10.5194/esd-4-219-2013.
- 866 Hoffman, F. M., and Coauthors, 2014: Causes and implications of persistent atmospheric
867 carbon dioxide biases in Earth System Models. *J. Geophys. Res. Biogeosciences*, **119**,
868 141–162, doi:10.1002/2013JG002381.
- 869 Holland, M. M., and C. M. Bitz, 2003: Polar amplification of climate change in coupled
870 models. *Clim. Dyn.*, **21**, 221–232, doi:10.1007/s00382-003-0332-6.
- 871 Hong, S.-Y., and E.-C. Chang, 2012: Spectral nudging sensitivity experiments in a regional
872 climate model. *Asia-Pac. J. Atmospheric Sci.*, **48**, 345–355, doi:10.1007/s13143-012-
873 0033-3.
- 874 van den Hurk, B., M. Best, P. Dirmeyer, A. Pitman, J. Polcher, and J. Santanello, 2011:
875 Acceleration of Land Surface Model Development over a Decade of Glass. *Bull. Am.*
876 *Meteorol. Soc.*, **92**, 1593–1600, doi:10.1175/BAMS-D-11-00007.1.
- 877 —, F. Doblas-Reyes, G. Balsamo, R. Koster, S. Seneviratne, and H. Camargo Jr, 2012: Soil
878 moisture effects on seasonal temperature and precipitation forecast scores in
879 Europe. *Clim. Dyn.*, **38**, 349–362, doi:10.1007/s00382-010-0956-2.
- 880 Jaeger, E. B., and S. I. Seneviratne, 2011: Impact of soil moisture–atmosphere coupling on
881 European climate extremes and trends in a regional climate model. *Clim. Dyn.*, **36**,
882 1919–1939, doi:10.1007/s00382-010-0780-8.



- 883 Jiafu Mao, and Coauthors, 2015: Disentangling climatic and anthropogenic controls on
884 global terrestrial evapotranspiration trends. *Environ. Res. Lett.*, **10**, 094008.
- 885 Jung, M., and Coauthors, 2010: Recent decline in the global land evapotranspiration trend
886 due to limited moisture supply. *Nature*, **467**, 951–954, doi:10.1038/nature09396.
- 887 Kim, H., 2010: *Role of rivers in the spatiotemporal variations of terrestrial hydrological*
888 *circulations*. University of Tokyo,.
- 889 Kim, H., P. J.-F. Yeh, T. Oki, and S. Kanae, 2009: Role of rivers in the seasonal variations of
890 terrestrial water storage over global basins. *Geophys. Res. Lett.*, **36**, n/a – n/a,
891 doi:10.1029/2009GL039006.
- 892 Koster, R. D., M. J. Suarez, and M. Heiser, 2000: Variance and Predictability of Precipitation
893 at Seasonal-to-Interannual Timescales. *J. Hydrometeorol.*, **1**, 26–46,
894 doi:10.1175/1525-7541(2000)001<0026:VAPOPA>2.0.CO;2.
- 895 —, and Coauthors, 2004: Regions of Strong Coupling Between Soil Moisture and
896 Precipitation. *Science*, **305**, 1138–1140, doi:10.1126/science.1100217.
- 897 Koster, R. D., and Coauthors, 2010a: Contribution of land surface initialization to
898 subseasonal forecast skill: First results from a multi-model experiment. *Geophys.*
899 *Res. Lett.*, **37**, L02402, doi:10.1029/2009GL041677.
- 900 Koster, R. D., S. P. P. Mahanama, B. Livneh, D. P. Lettenmaier, and R. H. Reichle, 2010b: Skill
901 in streamflow forecasts derived from large-scale estimates of soil moisture and
902 snow. *Nat. Geosci.*, **3**, 613–616, doi:10.1038/ngeo944.
- 903 Koven, C. D., W. J. Riley, and A. Stern, 2012: Analysis of Permafrost Thermal Dynamics and
904 Response to Climate Change in the CMIP5 Earth System Models. *J. Clim.*, **26**, 1877–
905 1900, doi:10.1175/JCLI-D-12-00228.1.
- 906 Lawrence, D. M., and Coauthors, submitted: The Land-Use Model Intercomparison Project
907 (LUMIP) experimental design. *Geosci Model Dev.*,
- 908 Lehning, M., 2013: Snow–atmosphere interactions and hydrological consequences. *Snow–*
909 *Atmosphere Interact. Hydrol. Consequences*, **55**, 1–3,
910 doi:10.1016/j.advwatres.2013.02.001.
- 911 Le Quere, C., M. R. Raupach, J. G. Canadell, and G. Marland et al., 2009: Trends in the
912 sources and sinks of carbon dioxide. *Nat. Geosci.*, **2**, 831–836, doi:10.1038/ngeo689.
- 913 Liu, Y. Y., W. A. Dorigo, R. M. Parinussa, R. A. M. de Jeu, W. Wagner, M. F. McCabe, J. P.
914 Evans, and A. I. J. M. van Dijk, 2012: Trend-preserving blending of passive and active
915 microwave soil moisture retrievals. *Remote Sens. Environ.*, **123**, 280–297,
916 doi:10.1016/j.rse.2012.03.014.



- 917 Materia, S., S. Gualdi, A. Navarra, and L. Terray, 2012: The effect of Congo River freshwater
918 discharge on Eastern Equatorial Atlantic climate variability. *Clim. Dyn.*, **39**, 2109–
919 2125, doi:10.1007/s00382-012-1514-x.
- 920 Meng, L., R. Paudel, P. G. M. Hess, and N. M. Mahowald, 2015: Seasonal and interannual
921 variability in wetland methane emissions simulated by CLM4Me' and CAM-chem and
922 comparisons to observations of concentrations. *Biogeosciences*, **12**, 4029–4049,
923 doi:10.5194/bg-12-4029-2015.
- 924 Mudryk, L. R., C. Derksen, P. J. Kushner, and R. Brown, 2015: Characterization of Northern
925 Hemisphere Snow Water Equivalent Datasets, 1981–2010. *J. Clim.*, **28**, 8037–8051,
926 doi:10.1175/JCLI-D-15-0229.1.
- 927 Mueller, B., and S. I. Seneviratne, 2014: Systematic land climate and evapotranspiration
928 biases in CMIP5 simulations. *Geophys. Res. Lett.*, **41**, 128–134,
929 doi:10.1002/2013GL058055.
- 930 —, and Coauthors, 2013: Benchmark products for land evapotranspiration: LandFlux-
931 EVAL multi-data set synthesis. *Hydrol Earth Syst Sci*, **17**, 3707–3720,
932 doi:10.5194/hess-17-3707-2013.
- 933 Mystakidis, S., E. L. Davin, N. Gruber, and S. I. Seneviratne, 2016: Constraining future
934 terrestrial carbon cycle projections using observation-based water and carbon flux
935 estimates. *Glob. Change Biol.*, n/a – n/a, doi:10.1111/gcb.13217.
- 936 Orth, R., and S. I. Seneviratne, submitted: Soil moisture and sea surface temperatures
937 similarly important for land climate in the warm season in the Community Earth
938 System Model. *J. Clim.*,.
- 939 Orth, R., R. D. Koster, and S. I. Seneviratne, 2013: Inferring Soil Moisture Memory from
940 Streamflow Observations Using a Simple Water Balance Model. *J. Hydrometeorol.*,
941 **14**, 1773–1790, doi:10.1175/JHM-D-12-099.1.
- 942 Peings, Y., H. Douville, R. Alkama, and B. Decharme, 2011: Snow contribution to springtime
943 atmospheric predictability over the second half of the twentieth century. *Clim. Dyn.*,
944 **37**, 985–1004, doi:10.1007/s00382-010-0884-1.
- 945 Perket, J., M. G. Flanner, and J. E. Kay, 2014: Diagnosing shortwave cryosphere radiative
946 effect and its 21st century evolution in CESM. *J. Geophys. Res. Atmospheres*, **119**,
947 1356–1362, doi:10.1002/2013JD021139.
- 948 Qu, X., and A. Hall, 2014: On the persistent spread in snow-albedo feedback. *Clim. Dyn.*, **42**,
949 69–81, doi:10.1007/s00382-013-1774-0.
- 950 Reager, J. T., A. S. Gardner, J. S. Famiglietti, D. N. Wiese, A. Eicker, and M.-H. Lo, 2016: A
951 decade of sea level rise slowed by climate-driven hydrology. *Science*, **351**, 699–703,
952 doi:10.1126/science.aad8386.



- 953 Rodell, M., I. Velicogna, and J. S. Famiglietti, 2009: Satellite-based estimates of groundwater
954 depletion in India. *Nature*, **460**, 999–1002, doi:10.1038/nature08238.
- 955 Seneviratne, S. I., D. Luthi, M. Litschi, and C. Schar, 2006: Land-atmosphere coupling and
956 climate change in Europe. *Nature*, **443**, 205–209, doi:10.1038/nature05095.
- 957 —, T. Corti, E. L. Davin, M. Hirschi, E. B. Jaeger, I. Lehner, B. Orlowsky, and A. J. Teuling,
958 2010: Investigating soil moisture–climate interactions in a changing climate: A
959 review. *Earth-Sci. Rev.*, **99**, 125–161, doi:10.1016/j.earscirev.2010.02.004.
- 960 —, and Coauthors, 2013: Impact of soil moisture–climate feedbacks on CMIP5 projections:
961 First results from the GLACE–CMIP5 experiment. *Geophys. Res. Lett.*, **40**,
962 2013GL057153, doi:10.1002/grl.50956.
- 963 Seneviratne, S. I., B. Van den Hurk, D. M. Lawrence, G. Krinner, G. Hurtt, H. Kim, C. Derksen,
964 and et al., 2014: Land Processes, Forcings, and Feedbacks in Climate Change
965 Simulations: The CMIP6 “LandMIPs.” *GEWEX Newsl.*, 6–10.
- 966 Seneviratne, S. I., M. G. Donat, A. J. Pitman, R. Knutti, and R. L. Wilby, 2016: Allowable CO2
967 emissions based on regional and impact-related climate targets. *Nature*, **529**, 477–
968 483.
- 969 Sheffield, J., G. Goteti, and E. F. Wood, 2006: Development of a 50-Year High-Resolution
970 Global Dataset of Meteorological Forcings for Land Surface Modeling. *J. Clim.*, **19**,
971 3088–3111, doi:10.1175/JCLI3790.1.
- 972 —, E. F. Wood, and M. L. Roderick, 2012: Little change in global drought over the past 60
973 years. *Nature*, **491**, 435–438, doi:10.1038/nature11575.
- 974 Singh, D., M. G. Flanner, and J. Perket, 2015: The global land shortwave cryosphere radiative
975 effect during the MODIS era. *The Cryosphere*, **9**, 2057–2070, doi:10.5194/tc-9-2057-
976 2015.
- 977 Sitch, S., and Coauthors, 2015: Recent trends and drivers of regional sources and sinks of
978 carbon dioxide. *Biogeosciences*, **12**, 653–679, doi:10.5194/bg-12-653-2015.
- 979 Thackeray, C. W., C. G. Fletcher, and C. Derksen, 2015a: Quantifying the skill of CMIP5
980 models in simulating seasonal albedo and snow cover evolution. *J. Geophys. Res.*
981 *Atmospheres*, **120**, 5831–5849, doi:10.1002/2015JD023325.
- 982 —, —, and —, 2015b: Quantifying the skill of CMIP5 models in simulating seasonal
983 albedo and snow cover evolution. *J. Geophys. Res. Atmospheres*, **120**, 5831–5849,
984 doi:10.1002/2015JD023325.
- 985 Thomas, J., A. Berg, and W. Merryfield, 2015: Influence of snow and soil moisture
986 initialization on sub-seasonal predictability and forecast skill in boreal spring. *Clim.*
987 *Dyn.*, 1–17, doi:10.1007/s00382-015-2821-9.



- 988 Trenberth, K. E., A. Dai, G. van der Schrier, P. D. Jones, J. Barichivich, K. R. Briffa, and J.
989 Sheffield, 2014: Global warming and changes in drought. *Nat. Clim Change*, **4**, 17–22.
- 990 Wada, Y., L. P. Beek, F. C. Sperna Weiland, B. F. Chao, Y. Wu, and M. F. Bierkens, 2012: Past
991 and future contribution of global groundwater depletion to sea-level rise. *Geophys.*
992 *Res. Lett.*, **39**.
- 993 Warszawski, L., K. Frieler, V. Huber, F. Piontek, O. Serdeczny, and J. Schewe, 2014: The Inter-
994 Sectoral Impact Model Intercomparison Project (ISI-MIP): Project framework. *Proc.*
995 *Natl. Acad. Sci.*, **111**, 3228–3232.
- 996 Watanabe, S., and Coauthors, 2014: Application of performance metrics to climate models
997 for projecting future river discharge in the Chao Phraya River basin. *Hydrol. Res.*
998 *Lett.*, **8**, 33–38, doi:10.3178/hrl.8.33.
- 999 Weedon, G. P., and Coauthors, 2011: Creation of the WATCH Forcing Data and Its Use to
1000 Assess Global and Regional Reference Crop Evaporation over Land during the
1001 Twentieth Century. *J. Hydrometeorol.*, **12**, 823–848, doi:10.1175/2011JHM1369.1.
- 1002 Weedon, G. P., G. Balsamo, N. Bellouin, S. Gomes, M. J. Best, and P. Viterbo, 2014: The
1003 WFDEI meteorological forcing data set: WATCH Forcing Data methodology applied to
1004 ERA-Interim reanalysis data. *Water Resour. Res.*, **50**, 7505–7514,
1005 doi:10.1002/2014WR015638.
- 1006 Wei, Y., and Coauthors, 2014: The North American Carbon Program Multi-scale Synthesis
1007 and Terrestrial Model Intercomparison Project – Part 2: Environmental driver data.
1008 *Geosci Model Dev*, **7**, 2875–2893, doi:10.5194/gmd-7-2875-2014.
- 1009 Xu, L., and Coauthors, 2013: Temperature and vegetation seasonality diminishment over
1010 northern lands. *Nat. Clim Change*, **3**, 581–586.
- 1011 Yoshimura, K., and M. Kanamitsu, 2008: Dynamical Global Downscaling of Global Reanalysis.
1012 *Mon. Weather Rev.*, **136**, 2983–2998, doi:10.1175/2008MWR2281.1.
- 1013 —, and —, 2013: Incremental Correction for the Dynamical Downscaling of Ensemble
1014 Mean Atmospheric Fields. *Mon. Weather Rev.*, **141**, 3087–3101, doi:10.1175/MWR-
1015 D-12-00271.1.
- 1016 Zampieri M, and Lionello P, 2011: Anthropic land use causes summer cooling in
1017 -Central Europe. *Clim. Res.*, **46**, 255–268.
- 1018 Zampieri, M., E. Serpetzoglou, E. N. Anagnostou, E. I. Nikolopoulos, and A. Papadopoulos,
1019 2012: Improving the representation of river–groundwater interactions in land
1020 surface modeling at the regional scale: Observational evidence and parameterization
1021 applied in the Community Land Model. *J. Hydrol.*, **420–421**, 72–86,
1022 doi:10.1016/j.jhydrol.2011.11.041.
- 1023 Zampieri, M., E. Scoccimarro, S. Gualdi, and A. Navarra, 2015: Observed shift towards earlier
1024 spring discharge in the main Alpine rivers. *Better Underst. Links Stress. Hazard*



- 1025 *Assess. Ecosyst. Serv. Water Scarcity*, **503–504**, 222–232,
1026 doi:10.1016/j.scitotenv.2014.06.036.
- 1027 Zhang, Y., and Coauthors, submitted: A Climate Data Record (CDR) for the global terrestrial
1028 water budget: 1984-2010. *J Clim.*,
- 1029 Zscheischler, J., R. Orth, and S. I. Seneviratne, 2015: A submonthly database for detecting
1030 changes in vegetation-atmosphere coupling. *Geophys. Res. Lett.*, **42**, 9816–9824,
1031 doi:10.1002/2015GL066563.
- 1032
- 1033

1034 **Annex: output data tables requested for LS3MIP**

1035

1036 *Table A1: Variable request table “LEday”: daily variables related to the energy cycle. Priority*1037 *index (p*) in column 1 indicates 1: “Mandatory” and 2: “Desirable”. The dimension (dim.)*1038 *column indicates T: time, Y: latitude, X: longitude, and Z: soil or snow layers.*

p*	name	standard_name (cf)	long_name (netCDF)	unit	direction	dim.
1	rss	surface_net_downward_shortwave_flux	Net shortwave radiation	W/m ²	Downward	TYX
1	rls	surface_net_downward_longwave_flux	Net longwave radiation	W/m ²	Downward	TYX
2	rsds	surface_downwelling_shortwave_flux_in_air	Downward short-wave radiation	W/m ²	Downward	TYX
2	rlds	surface_downwelling_longwave_flux_in_air	Downward long-wave radiation	W/m ²	Downward	TYX
2	rsus	surface_upwelling_shortwave_flux_in_air	Upward short-wave radiation	W/m ²	Upward	TYX
2	rlus	surface_upwelling_longwave_flux_in_air	Upward long-wave radiation	W/m ²	Upward	TYX
1	hfls	surface_upward_latent_heat_flux	Latent heat flux	W/m ²	Upward	TYX
1	hfss	surface_upward_sensible_heat_flux	Sensible heat flux	W/m ²	Upward	TYX
1	hfds	surface_downward_heat_flux	Ground heat flux	W/m ²	Downward	TYX
1	hfdsn	surface_downward_heat_flux_in_snow	Downward heat flux into snow	W/m ²	Downward	TYX
2	hfmlt	surface_snow_and_ice_melt_heat_flux	Energy of fusion	W/m ²	Soild to Liquid	TYX
2	hfsbl	surface_snow_and_ice_sublimation_heat_flux	Energy of sublimation	W/m ²	Soild to Vapor	TYX
2	tau	surface_downward_stress	Momentum flux	N/m ²	Downward	TYX
2	hfrs	temperature_flux_due_to_rainfall_expressed_as_heat_flux_onto_snow_and_ice	Heat transferred to snowpack by rainfall	W/m ²	Downward	TYX
1	dtes	change_over_time_in_thermal_energy_content_of_surface	Change in surface heat storage	J/m ²	Increase	TYX
1	dtesn	change_over_time_in_thermal_energy_content_of_surface_snow_and_ice	Change in snow/ice cold content	J/m ²	Increase	TYX
1	ts	surface_temperature	Average surface temperature	K	-	TYX
2	tsns	surface_snow_skin_temperature	Snow Surface Temperature	K	-	TYX
2	tcs	surface_canopy_skin_temperature	Vegetation Canopy Temperature	K	-	TYX
2	tgs	surface_ground_skin_temperature	Temperature of bare soil	K	-	TYX
2	tr	surface_radiative_temperature	Surface Radiative Temperature	K	-	TYX
1	albs	surface_albedo	Surface Albedo	-	-	TYX
1	albsn	snow_and_ice_albedo	Snow Albedo	-	-	TYX
1	snc	surface_snow_area_fraction	Snow covered fraction	-	-	TYX



2	albc	canopy_albedo	Canopy Albedo	-	-	TYX
2	cnc	surface_canopy_area_fraction	Canopy covered fraction	-	-	TYX
1	tsl	soil_temperature	Average layer soil temperature	K	-	TZYX
1	tsnl	snow_temperature	Temperature profile in the snow	K	-	TZYX
1	tasmax	air_temperature_maximum	Daily Maximum Near-Surface Air Temperature	K	-	TYX
1	tasmin	air_temperature_minimum	Daily Minimum Near-Surface Air Temperature	K	-	TYX
2	clt	cloud_area_fraction	Total cloud fraction	-	-	TYX

1039



1040 *Table A2: Variable request table “LWday”: daily variables related to the water cycle.*

p*	name	standard_name (cf)	long_name (netCDF)	unit	direction	dim.
1	pr	precipitation_flux	Precipitation rate	kg/m ² /s	Downward	TYX
2	prra	rainfall_flux	Rainfall rate	kg/m ² /s	Downward	TYX
2	prsn	snowfall_flux	Snowfall rate	kg/m ² /s	Downward	TYX
2	prrc	convective_rainfall_flux	Convective Rainfall rate	kg/m ² /s	Downward	TYX
2	prsn	convective_snowfall_flux	Convective Snowfall rate	kg/m ² /s	Downward	TYX
1	prveg	precipitation_flux_onto_canopy	Precipitation onto canopy	kg/m ² /s	Downward	TYX
1	et	surface_evapotranspiration	Total Evapotranspiration	kg/m ² /s	Upward	TYX
1	ec	liquid_water_evaporation_flux_from_canopy	Interception evaporation	kg/m ² /s	Upward	TYX
1	tran	Transpiration	Vegetation transpiration	kg/m ² /s	Upward	TYX
1	es	liquid_water_evaporation_flux_from_soil	Bare soil evaporation	kg/m ² /s	Upward	TYX
2	eow	liquid_water_evaporation_flux_from_open_water	Open water evaporation	kg/m ² /s	Upward	TYX
2	esn	liquid_water_evaporation_flux_from_surface_snow	Snow Evaporation	kg/m ² /s	Upward	TYX
2	sbl	surface_snow_and_ice_sublimation_flux	Snow sublimation	kg/m ² /s	Upward	TYX
2	slbnosn	sublimation_amount_assuming_no_snow	Sublimation of the snow free area	kg/m ² /s	Upward	TYX
2	potet	water_potential_evapotranspiration_flux	Potential Evapotranspiration	kg/m ² /s	Upward	TYX
1	mrro	runoff_flux	Total runoff	kg/m ² /s	Out	TYX
2	mrros	surface_runoff_flux	Surface runoff	kg/m ² /s	Out	TYX
1	mrrob	subsurface_runoff_flux	Subsurface runoff	kg/m ² /s	Out	TYX
1	snm	surface_snow_and_ice_melt_flux	Snowmelt	kg/m ² /s	Solid to liquid	TYX
1	snrefr	surface_snow_and_ice_refreezing_flux	Re-freezing of water in the snow	kg/m ² /s	Liquid to solid	TYX
2	snmsl	surface_snow_melt_flux_into_soil_layer	Water flowing out of snowpack	kg/m ² /s	Out	TYX
2	qgwr	water_flux_from_soil_layer_to_groundwater	Groundwater recharge from soil layer	kg/m ² /s	Out	TYX
2	rivo	water_flux_from_upstream	River Inflow	m ³ /s	In	TYX
2	rivi	water_flux_to_downstream	River Discharge	m ³ /s	Out	TYX
1	dslw	change_over_time_in_water_content_of_soil_layer	Change in soil moisture	kg/m ²	Increase	TYX
1	dsn	change_over_time_in_surface_snow_and_ice_amount	Change in snow water equivalent	kg/m ²	Increase	TYX
1	dsw	change_over_time_in_surface_water_amount	Change in Surface Water Storage	kg/m ²	Increase	TYX
1	dcw	change_over_time_in_canopy_water_amount	Change in interception storage	kg/m ²	Increase	TYX



2	dgw	change_over_time_in_groundwater	Change in groundwater	kg/m ²	Increase	TYX
2	drivw	change_over_time_in_river_water_amount	Change in river storage	kg/m ²	Increase	TYX
1	rzwc	water_content_of_root_zone	Root zone soil moisture	kg/m ²	-	TYX
1	cw	canopy_water_amount	Total canopy water storage	kg/m ²	-	TYX
1	snw	surface_snow_amount	Snow Water Equivalent	kg/m ²	-	TZYX
1	snwc	canopy_snow_amount	SWE intercepted by the vegetation	kg/m ²	-	TYX
2	lwsnl	liquid_water_content_of_snow_layer	Liquid water in snow pack	kg/m ²	-	TZYX
1	sw	surface_water_amount_assuming_no_snow	Surface Water Storage	kg/m ²	-	TYX
1	mrlsl	moisture_content_of_soil_layer	Average layer soil moisture	kg/m ²	-	TZYX
1	mrsos	moisture_content_of_soil_layer	Moisture in top soil (10cm) layer	kg/m ²	-	TYX
1	mrsow	relative_soil_moisture_content_above_field_capacity	Total Soil Wetness	-	-	TYX
2	wtd	depth_of_soil_moisture_saturation	Water table depth	m	-	TYX
1	tws	canopy_and_surface_and_subsurface_water_amount	Terrestrial Water Storage	kg/m ²	-	TYX
2	mrlqso	mass_fraction_of_unfrozen_water_in_soil_layer	Average layer fraction of liquid moisture	-	-	TZYX
1	mrfsofr	mass_fraction_of_frozen_water_in_soil_layer	Average layer fraction of frozen moisture	-	-	TZYX
2	prrsn	mass_fraction_of_rainfall_onto_snow	Fraction of rainfall on snow.	-	-	TYX
2	prnsn	mass_fraction_of_snowfall_onto_snow	Fraction of snowfall on snow.	-	-	TYX
1	lqsn	mass_fraction_of_liquid_water_in_snow	Snow liquid fraction	-	-	TZYX
1	snd	surface_snow_thickness	Depth of snow layer	m	-	TYX
1	agesno	age_of_surface_snow	Snow Age	day	-	TYX
2	sootsn	soot_content_of_surface_snow	Snow Soot Content	kg/m ²	-	TYX
2	sic	sea_ice_area_fraction	Ice-covered fraction	-	-	TYX
2	sit	sea_ice_thickness	Sea-ice thickness	m	-	TYX
2	dfr	depth_of_frozen_soil	Frozen soil depth	m	Downward	TYX
2	dmlt	depth_of_subsurface_melting	Depth to soil thaw	m	Downward	TYX
2	tpf	permafrost_layer_thickness	Permafrost Layer Thickness	m	-	TYX
2	pflw	liquid_water_content_of_permafrost_layer	Liquid water content of permafrost layer	kg/m ²	-	TYX
			Aerodynamic conductance	m/s	-	TYX
2	ares	aerodynamic_resistance	Aerodynamic resistance	s/m	-	TYX
1	hur	relative_humidity	Relative humidity	%	-	TYX
1	hurmax	relative_humidity_maximum	Daily Maximum Near-Surface Relative Humidity	%	-	TYX
1	hurmin	relative_humidity_minimum	Daily Minimum Near-Surface Relative Humidity	%	-	TYX



1042 *Table A3: Variable request table “LCmon”: monthly variables related to the carbon cycle.*

P*	name	standard_name (cf)	long_name (netCDF)	unit	direction	dim.
1	gpp	gross_primary_productivity_of_carbon	Gross Primary Production	Kg/m ² /s	Downward	TYX
1	npp	net_primary_productivity_of_carbon	Net Primary Production	Kg/m ² /s	Downward	TYX
1	nep	surface_net_downward_mass_flux_of_carbon_dioxide_expressed_as_carbon_due_to_all_land_processes_excluding_anthropogenic_land_use_change	Net Ecosystem Exchange	Kg/m ² /s	Downward	TYX
1	ra	plant_respiration_carbon_flux	Autotrophic Respiration	Kg/m ² /s	Upward	TYX
1	rh	heterotrophic_respiration_carbon_flux	Heterotrophic Respiration	Kg/m ² /s	Upward	TYX
1	fLuc	surface_net_upward_mass_flux_of_carbon_dioxide_expressed_as_carbon_due_to_emission_from_anthropogenic_land_use_change	Net Carbon Mass Flux into Atmosphere due to Land Use Change	Kg/m ² /s	Upward	TYX
1	cSoil	soil_carbon_content	Carbon Mass in Soil Pool	Kg/m ²	-	TYX
1	cLitter	litter_carbon_content	Carbon Mass in Litter Pool	Kg/m ²	-	TYX
1	cVeg	vegetation_carbon_content	Carbon Mass in Vegetation	Kg/m ²	-	TYX
1	cProduct	carbon_content_of_products_of_anthropogenic_land_use_change	Carbon Mass in Products of Land Use Change	Kg/m ²	-	TYX
2	cLeaf	leaf_carbon_content	Carbon Mass in Leaves	Kg/m ²	-	TYX
2	cWood	wood_carbon_content	Carbon Mass in Wood	Kg/m ²	-	TYX
2	cRoot	root_carbon_content	Carbon Mass in Roots	Kg/m ²	-	TYX
2	cMisc	miscellaneous_living_matter_carbon_content	Carbon Mass in Other Living Compartments on Land	Kg/m ²	-	TYX
2	fVegLitter	litter_carbon_flux	Total Carbon Mass Flux from Vegetation to Litter	Kg/m ² /s	-	TYX
2	fLitterSoil	carbon_mass_flux_into_soil_from_litter	Total Carbon Mass Flux from Litter to Soil	Kg/m ² /s	-	TYX
2	fVegSoil	carbon_mass_flux_into_soil_from_vegetation_excluding_litter	Total Carbon Mass Flux from Vegetation Directly to Soil	Kg/m ² /s	-	TYX
1	treeFrac	area_fraction	Tree Cover Fraction	%	-	TYX
1	grassFrac	area_fraction	Natural Grass Fraction	%	-	TYX
1	shrubFrac	area_fraction	Shrub Fraction	%	-	TYX
1	cropFrac	area_fraction	Crop Fraction	%	-	TYX
1	pastureFrac	area_fraction	Anthropogenic Pasture Fraction	%	-	TYX



1	baresoilFrac	area_fraction	Bare Soil Fraction	%	-	TYX
1	residualFrac	area_fraction	Fraction of Grid Cell that is Land but Neither Vegetation-Covered nor Bare Soil	%	-	TYX
1	lai	leaf_area_index	Leaf Area Index	Kg/m ²	-	TYX

1043



1044 *Table A4: Variable request table “L3hr”: 3-hourly variables to generate the atmospheric*
 1045 *boundary conditions for the off-line simulation.*

p*	name	standard_name (cf)	long_name (netCDF)	unit	direction	dim.
1	rsds	surface_downwelling_shortwave_flux_in_air	Downward short-wave radiation	W/m ²	Downward	TYX
1	rlds	surface_downwelling_longwave_flux_in_air	Downward long-wave radiation	W/m ²	Downward	TYX
1	hus	specific_humidity	Near surface specific humidity	kg/kg	-	TYX
1	ta	air_temperature	Near surface air temperature	K	-	TYX
1	ps	surface_air_pressure	Surface Pressure	Pa	-	TYX
1	ws	wind_speed	Near surface wind speed	m/s	-	TYX
2	va	northward_wind	Near surface northward wind component	m/s	Northward	TYX
2	ua	eastward_wind	Near surface eastward wind component	m/s	Eastward	TYX
2	pr	precipitation_flux	Precipitation rate	kg/m ² /s	Downward	TYX
1	prra	rainfall_flux	Rainfall rate	kg/m ² /s	Downward	TYX
1	prsn	snowfall_flux	Snowfall rate	kg/m ² /s	Downward	TYX
2	prrc	convective_rainfall_flux	Convective Rainfall rate	kg/m ² /s	Downward	TYX
2	prsn	convective_snowfall_flux	Convective Snowfall rate	kg/m ² /s	Downward	TYX
1	clt	cloud_area_fraction	Total cloud fraction	-	-	TYX
2	co2c	mole_fraction_of_carbon_dioxide_in_air	Near surface CO2 concentration	-	-	TYX

1046

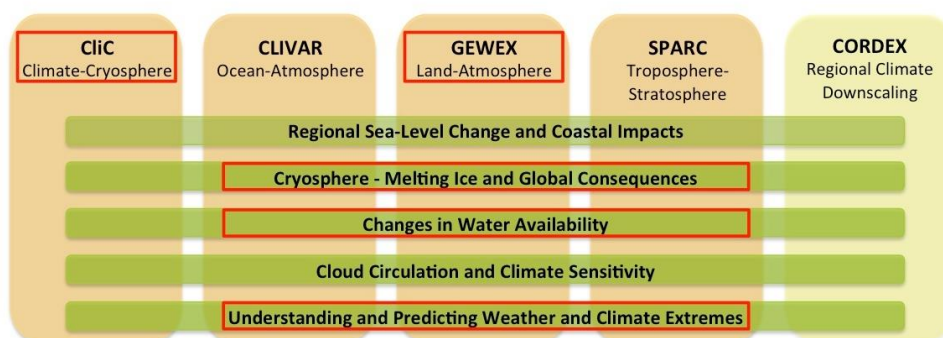
1047



1048 **Figures**

1049

LS3MIP within WCRP Core Projects and Grand Challenges

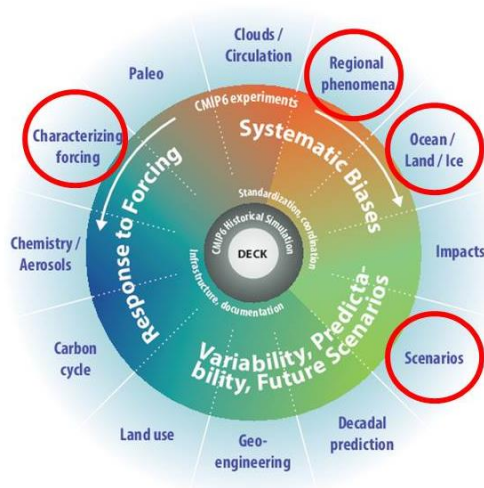


1050

Figure 1: Relevance of LS3MIP for WCRP Core Projects and Grand Challenges¹⁹

1051

1052

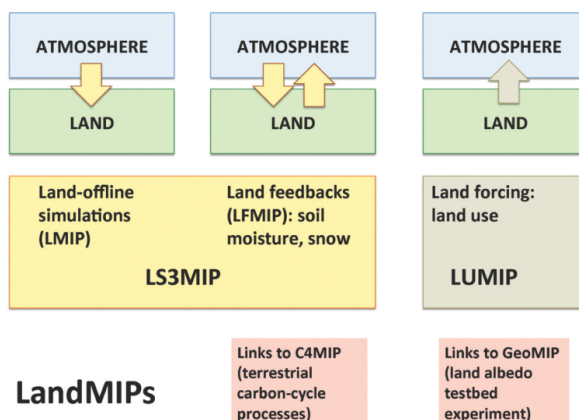


1053

Figure 2: Embedding of LS3MIP within CMIP6. Adapted from Eyring et al. (2015)

1054

¹⁹ <http://wcrp-climate.org/index.php/grand-challenges>; status Dec 2015



1055

1056 *Figure 3: Structure of the “LandMIPs”. LS3MIP includes (1) the offline representation of land*
 1057 *processes (LMIP) and (2) the representation of land-atmosphere feedbacks related to snow*
 1058 *and soil moisture (LFMIP). Forcing associated with land use is assessed in LUMIP. Substantial*
 1059 *links also exist to C4MIP (terrestrial carbon cycle). Furthermore, a land albedo testbed*
 1060 *experiment is planned within GeoMIP. From Seneviratne et al. (2014)*

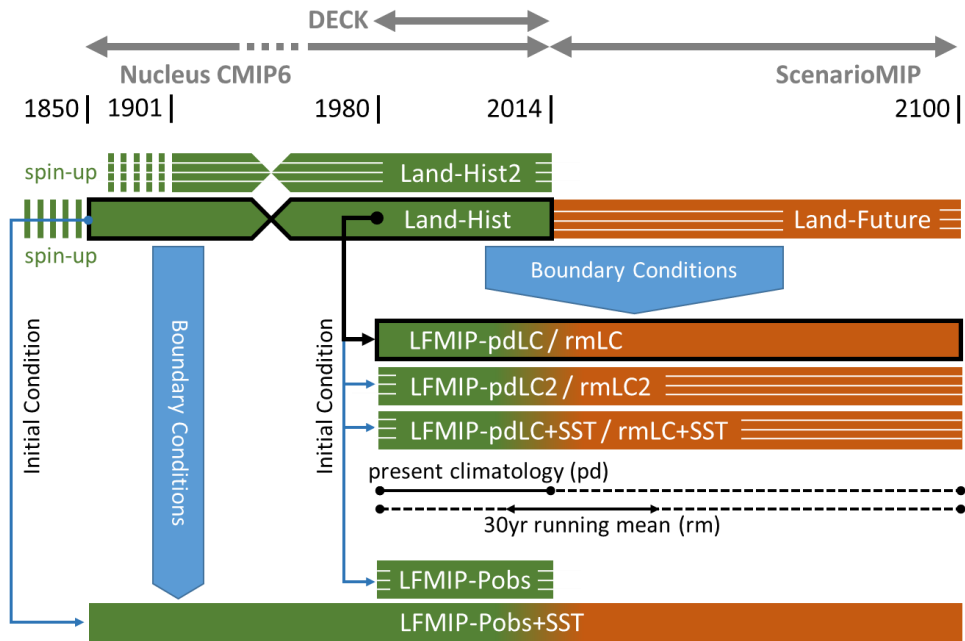
1061

1062

1063

1064

1065



1066

1067

1068

1069

1070

1071

1072

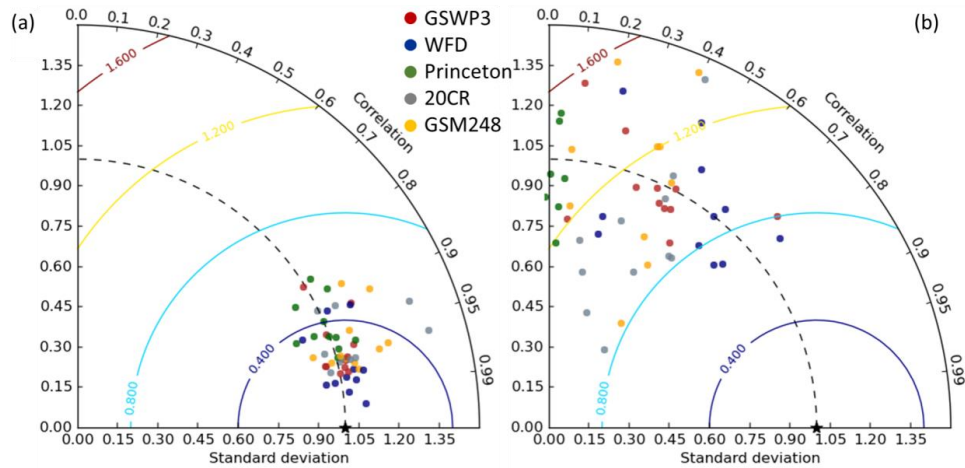
1073

1074

1075

1076

Figure 4: Schematic diagram for the experiment structure of LS3MIP. Tier 1 experiments are indicated with a heavy black outline, and complementary ensemble experiments are indicated with white hatched lines. For details on the experiments and acronyms, see Table 1 and text.



1077

1078

Figure 5: Taylor diagram for evaluating the forcing datasets comparing to daily observations from FLUXNET sites: (a) 2m air temperature and (b) precipitation. Red, blue, and green dots indicate GSWP3, Watch Forcing Data (Weedon et al. 2011) and Princeton forcing (Sheffield et al. 2006), respectively. Grey and orange dots indicate 20CR and its dynamically downscaled product (GSM248).

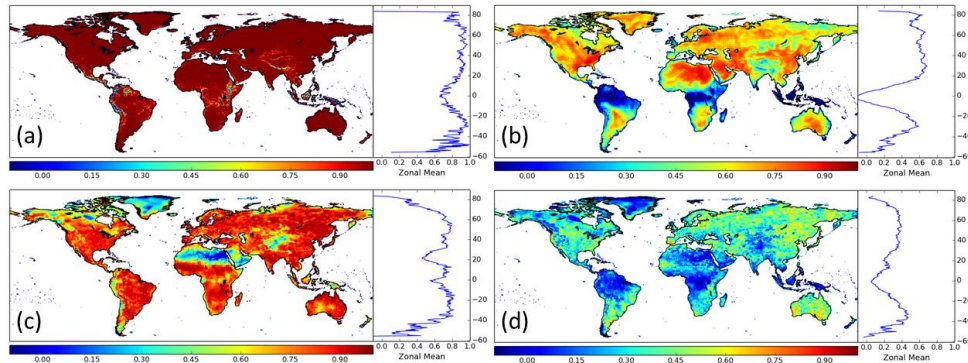
1079

1080

1081

1082

1083



1084

1085

Figure 6: Global distributions of the similarity index (Ω) for 2001-2010 of monthly mean (a, c) and (b, d) monthly variance (calculated from daily data from each data set) of 2m air temperature (top panels) and precipitation (bottom panels), respectively. Shown are global distributions and zonal means. After (Kim 2010).

1086

1087

1088

1089